Editor's comments

Author's response in red

P1L20: SMN -> SMB. Also, sensitivity of what? Done (P1L19)

P1L22: "120-m-long" Done, although the website http://www.the-cryosphere.net/for_authors/manuscript_preparation.html indicates: "It is our house standard not to hyphenate modifiers containing abbreviated units (e.g. "3-m stick" should be "3m stick"). This also applies to the other side of the hyphenated term (e.g. "3m long rope", not "3-m-long rope")."

P1L23: DML is not used in the abstract. Done (P1L22)

P1L26: The bottom of the ice core is dated as 1759 +/- 16 AD, so that the ice core includes the climate proxies in the past 240 years, not only in the 20th century as it is said in the manuscript title and at the end of the abstract (20th and 21st centuries).

With our uncertainty range, we can say that the increase likely starts in the early 20th century and very likely in the mid-20th century, and is continuing in the 21st century. The title and the abstract summarize this main finding of the paper.

P1L32: What does "in at least the last 50 years" mean? I think that the authors want to say "Reconstructed SMB increases with time in the last 50 years by 30%" or "Reconstructed SMB increases with time, and this trend becomes even clearer in the past 50 years". Done (P1L28)

P2L11: see my comment above about "20th and 21st centuries." Same answer as above

P2L18: remove "coastal". Ice discharge always happens at the coast. Done (P2L11)

P2L21: balanced -> compensated? Done (P2L14)

P3L20 -24: Please rewrite these new sentences. In particular, I have no idea what "with high SMB" means at the line 21. Done (P3L27)

P4L2: "120-m-long" Done (P4L27)

P4L8: remove ", including DML," Done (P5L3)

P4L14-15: "preliminary ice core analysis" refers an earlier work of what is reported in this manuscript, I believe. So, it is not appropriate to cite that result in this way. Is it possible to show stake-measured SMB instead (as it is independent of the ice core work reported here)?

This sentence has been removed. It was indeed the value derived from early ice core analysis, which was not published at that time but has been used in Drews et al. (2015) and Callens et al. (2016). (P5L8-9)

P4L26: Change to "Radar stratigraphy shows that locally maximum SMB happens about 4 km upwind of the ice core site"? And consider adding a figure showing the ice core site together with layer-depth SMB and surface elevations in contours (similar to Fig. 4 of Drews et al., 2015).

Done the former (P5L20). Both the ice core position and layer-depth SMB and surface elevations are available in Figs. 1 and 4 of Drews et al. (2015) so we are not convinced that a figure is necessary.

P7L5-10: Because Kjær et al. is still under review, please include sentences that describe the magnitude of this correction. I assume that this method removes long-term trends but not short-term variations so that determining annual cycles in the ECM record is not sensitively affected by this correction. Also, it is hard to match depths of the ice core and borehole (Hubbard et al., 2013) precisely (Reviewer pointed out this issue but the authors did not respond clearly).
Kjær et al., 2016 is now published online. These sentences have been reworded (P7L20-22). However, note that we actually do not use the televiewer log depth scale because we only use the best fit on gravimetric density.

P7L28: change to "and rheological anisotropy of the ice. The strain rates are insensitive to the surface thinning and the strain rates remain the same even if the surface elevation is kept uniform in the model" or such. Also, be more specific which Drews's model result is used here. I think you used "A(n=3), dH = 100, chi = 0.03 m/a, layer-depth SMB, (anisotropic rheology)" in Fig. 11 of Drews et al.
Reworded to: "The magnitude of applied surface lowering is small and does not alter the strain rates significantly compared to a steady-state scenario" (P8L9-11)

P7L29: change to "Separately, we used GPS data to derive the horizontal strain on the surface."
Reworded to add more precision. (P8L11)

P7L30: change "0.002 a-1" to "2 x 10-3 a-1" Done (P8L14)

P8L1: What does "scaled" mean here? Do you mean "The vertical strain rates derived by Drews et al. (2015) is xx so we increased (or decreased?) Drews's vertical strain rate by xx uniformly"?? Even with this change, it is unclear what "best fit" means (if Drews's profile is simply shifted, not shape of the depth function is changed).
This sentence has now been reworded (P8L14-17). Scaled means that the shape of the vertical velocity profile was used and scaled to the long-term accumulation rate, since a lower acc. rate was used by Drews. Since the shape of the profile determines ε_{zz} (and not the absolute values), this can be safely done.

P8L7: Change "alternatively" to "The other method we used to derive the vertical thinning rates is …." Done (P8L18)

P8L12-13: Figure 2b shows that Drews et al. and DJ model show distinct e_zz over the ice-core depths. They are different by ~13%. Is it significant for your discussion, i.e. do you need to develop the historical SMB records each for Drews's strain rate and for DJ strain rate?
It is shown in Fig. 6 that this difference in strain rate does not affect the historical SMB records, as the curves corrected with both corrections are overlaying. It was hard to see the green line in Fig 6a because the black line appears on top, so we made the green line thicker.

P8L15: do you mean "We used Drews's and DJ's strain rates to compensate dynamic thinning in the annual layer thickness in order to estimate past SMB."? Done (P8L26-29).

P9L11: Please add a sentence to describe how this model is used in this paper. Done (P9L2-3).

P9L26: What do you mean by "trend"? Is it east-west trend, temporal trend?? Done (P9L17).

P10L7: change to "These properties change smoothly over a few very thin ice layers (white dots in Fig. 3) so we assume that they are not disturbed by surface melting". Rewritten close to suggested (P9L25).

P10L22: change to “the reference surface (November 2012 AD)” Done (P10L10).

P10L23: change to “correspondingly dated to 1775 AD and 1743, respectively, or 1758 +/- 16 AD.” (the mean of 1775 and 1743 is 1759, not 1758, but I assume that this difference is related to the timing of the drilling in 2012). Done (P10L11-12)

P10L28: Do you want to say “Hereafter, we examine volcanic signals in ECM signals as possible age controls to more precisely develop the depth-age scale bounded by the oldest and youngest cases.” Done (P10L17-18).

P11L9: Be careful to say “threshold”. If I understand correctly, the authors want to say “the preliminary depth-age scale developed with layer counting shows that the largest ECM peak beyond 4 sigma presents at 1815 so we interpreted it as the Tambora eruption. The secondary peak associated with the Tambora peak is found as well (unknown source, 1809) but its ECM peak reaches only 2 sigma. This ECM peak is lower than those found in most ice cores [ref] but still in a range of previously reported values [ref]. We found 13 other ECM peaks beyond 2 sigma, which can be potentially matched with known volcanic events. Nevertheless, there are many other ECM peaks beyond 2 sigma as well. So, we conclude ….”. Rewritten close to suggested (P10L25-P11-L6)

P11L17: “absolute”, not “relative”? I believe that the authors say that the absolute dating using volcanic eruptions remain uncertain. Reworded (P11L4).

P11L19: The response letter says that the authors prefer the oldest estimate. If it is the case, develop the argument here further and say something like “We believe that the oldest depth-age scale is more realistic than the youngest estimate because of matching with the Tambora eruption, though it is not really convincing. Therefore, we use …” Done (P10L27)

P12L6: Add thinning rate corrections. Done (P11L19)

P12L8: The authors said that they cannot conclude whether the young or old depth-age scales are better, but the age of the ice-core bottom shown here (1744) is probably tied to the oldest estimate (but if so, it would be 1743 not 1744). Also, Why is the youngest age in the core changed to 201 from November 2012? Changed to: from 1759 ± 16 years to November 2012 (P11L20)

P12L9: move the sentence “without correction for layer thinning” above so that you report the layer thickness first, and then derived SMB. Also, show the range of annual layer thickness (max, min, mean), instead of just reporting the mean value. Done (P12L8-9)

P12L12: I got confused. The paragraph immediately above reports the derived SMB, so I assume that the thinning corrections are already made. Please reorganize paragraphs in Section 3.2 to clearly demonstrate the logical flow. Done

P12L14: Is it really Section 4.2 (Discussion)? If so, it’s better to say something like “we discuss this point further in Section 4.2.” No, it was 2.4 (corrected, P11L28)

P12L28-30: Remove the sentence about dynamic thinning; it is obvious and rather confusing. You just say here that the layer has been thinned, not thickened. Done

P13: see comments to Table 1. Consider moving these paragraphs about averaged SMB values to a discussion session where you compare these values to previous studies.
The comparison to previous studies is discussed with Figure 9. In the discussion, it is not our goal to compare the absolute values but only the trends. However, we think it is important to provide the values we use to calculate our trends and that this is part of the results section.

P14L4: add "~240 years" after "the whole period" Done (P12L28)

P14L6: change to SMB. Done (P13L2)

P14L8: "bounded", instead of "determined"? The real SMB is expected to be somewhere between the oldest and youngest estimates. Done (P13L6)

P14L11: Here you explain the error bars in Figure 6, but the explanation is too brief to give a comprehensive idea what they are. If I understand correctly, the authors assume that the summer peak can be shifted up to 5 cm to both sides. In other words, if the annual layer is A cm thick, the thickest possible layer can be A + 10 cm (5 cm widen to both sides), and the thinnest possible layer can be A - 10 cm. Then you applied the thinning factor to estimate the uncertainty of the estimated SMB value. Do I understand correctly? However, if this is the case, the error bar is shorter when the SMB value is small, and it is longer otherwise. I cannot such feature in Figure 6.
There was indeed a mistake in the way individual error bars were calculated. They are now calculated the way the Editor describes (except the error is reduced to 5 cm below 85 m because the resolution of water stable isotopes measurements increases). The explanation is now given in the text (P12L5-7).

P14L11-13: I cannot understand this argument. Consistent features between isotopes and ions support an hypothesis that both represent seasonal changes. However, because both were sampled by 5 cm or 10 cm, both depth profiles may overlook an annual cycle that appears less than 5 cm thick. Uncorrected layer thickness (orange curve in Fig. 6a) shows that it is unlikely to miss such thin annual layers, but similarity of isotope and ion profiles cannot be the evidence for this argument.
We thank the Editor for pointing this out and we have reworded (P13L8-14).

P14L22: Provide reference/status of this paper. Done (P13L25).

P15L6ff: "in the vicinity of the crest"; topographic feature (Crest), not ice-flow feature (divide), should be cited in terms of SMB's spatial pattern. I saw that "divide" is used at some other places as well; please correct them as well. Replaced, unless we specifically refer to the ice flow feature, when mentioning Raymond effect.

P15L7: Drews et al. did not exclude a possibility of recent crest migration, which is too young to deform the Raymond Arches found at depths greater than 50-100 m where Raymond Arches become more visible.
Reworded (P14L9-19).

P15L21: here you say that the ice-core-derived results are compared with two climate models, but later you compare the results with ERA-Interim, RACMO2, and CESM. Amended (P14L21).

P15 L25: replace R2 with correlation coefficient or such. Done (P14L24-25).

P15L30: please add more information to explain why a freely-evoluting model output cannot be compared directly but still your discussion here can be valid. We added to Section 2.5: Because CESM is not bound by observations, and is a freely evolving model that generates its own climate, the simulated SMB time series cannot be directly compared to the observed one. Instead we use a statistical approach: we use the historical time series of CESM…."

P16L1: CESM output of the SMB mentioned here (0.295) is an average value for a certain period or the most recent SMB in 2011?
This is the average of the historical period, i.e. 1850-2005. We added this to the text (P14L28).

P16L11: How many days is this region covered with sea ice? This information is necessary to judge how 20-40 days fewer sea ice coverage is significant.
That varies widely, from ~120 days in the northern part to > 200 days in the southern part. We changed this line to:
"sea ice coverage is substantially lower than average (20–40 fewer days with sea-ice cover, **i.e. about 10-30% reduction compared to the average of 120-200 days**, Fig 8)" (P15L7).

P17ff: Section 4.1 shows many numbers and it is very hard to keep tracking the main argument. Please carefully review this section and re-organize it so that the discussion can be presented more clearly. Done.

P17L23: Drews's Figures 3b and 7 shows that anomalously low SMB is persistent at the current position to the age of ice at 60 m depth. This is I think support evidence of author's argument that the observed trend of SMB in the ice core presents the temporal changes, not migrating spatial patterns. Done (P14L17-19).

P20L6: change accumulation to SMB. Done (P17L14).

P20L9: indicate the name of these two coastal sites that show significant increase of SMB in the last 20 years compared to the last 200 years. Done (P17L17).

P20L13: change "less important" to "insignificant" or "less visible". Done (P17L18).

P21L28: remove "2009 and 2011" so it will be "than average SMB years (Table 2)." Done (P18L8)

P22L15: It is said that detrended dataset is not shown, but the authors presented 11-year running mean SMB (Figure 6). Is this running mean record good enough to identify anomalous events in 2-4 years (1991-95 and 1940-42)?
No, the running mean is not sufficient so we reworded to: "our record does not support this observation." (P18L21).

P24L11: "A 120-m-long", change "divide" to "summit" or "ridge (or crest)". Done (P19L17)

P24L14: "Therefore we counted annual layers to develop oldest and youngest estimates of the ice. The annual layer thickness, density, and thinning functions are applied to derive time series of SMB from annual layer thicknesses." Reworded closely (P19L19-22).

P24L20: do you mean that "wind re-distribution is significant near the ice -core site but it is likely that this effect is persistent over time so that ice-core records represent SMB time series rather than migrating spatial patterns of SMB"? Reworded closely (P19L26-P20L1).

P24L25-27: I cannot agree. Probably you want to say “Neither currently available climate models and re-analysis data cannot resolve ice-rise topography so their predictions are hard to match with the ice-core-derived SMB. Nevertheless, their temporal trends can be compared, and ….” Done (P20L9-14).

P25L10: I believe that the authors can be more confident about their results. Clear seasonal cycles (not only thin ice layers!) found in this ice core clearly demonstrated the potential of a deep core from this site as excellent paleoclimate proxies. Done (P20L18).

P25L21: Change “uncorrected SMB” to “annual layer thickness in ice”? “uncorrected SMB” sounds quite confusing. Done (P20L24).

Table 1

- I am not really sure how these average values for different periods are important. You said that it is for comparison with other studies and if so please consider adding an extra column showing the SMB values obtained from previous studies and compared with the average values that you are reporting.

These values from previous studies are shown in Table A1. It is now mentioned in Table 1 caption: ‘These values may be compared with those of several published studies, summarized in Table A1’.

Figure 1

- Change “accumulation” in the figure to “SMB”. Done.

Figure 3

- Add something like “d18O profiles are shown multiple times to better illustrate correlations between d18O and major ion profiles”. Done.

Figure 5

- It’s very hard to see thin gray bands. Use more distinct color (red, blue, or such, not gray). Done.

Figure 6

- Please align all four panels vertically so each panel can be a bit wider for full one-column width, and it is easier to compare time series. When I saw these panels first time, I had an impression that panels a and b are paired and c and d are paired. Done.

- What do error bars in panels b and c show?

They now show error on individual annual layer thickness calculated as 5-10 cm error (depending on water stable isotopes resolution) converted to m w.e.. This is now mentioned in the caption and in the text (P12L5-7)

- How is the uncertainty range (panel d) derived? Please explain more clearly in the main text.

It is the uncertainty range bounded by the youngest and the oldest estimates for 11 year running means. It is now stated in the text (P12L7-8).

Figure 7

- Distinguish curve and line in the caption. Pink and blue are curves, while black one is a line.

Done

- Please rewrite this caption; it is quite confusing. I believe that three datasets are normalized to their average values for the 1084-2000 period and their temporal variations are shown relative to those average values. I believe that “1979-1989” and “1850-2011” are typos.

The temporal coverage being different for the three datasets, as well as their absolute SMB values, we chose the most recent 11 years period common to the three datasets (1979-1989) to see how these 11 year running means compare with each other in terms of trends. 1850-2011 is the period of overlap between CESM and our ice core data.

Figure 8
- The caption is confusing. I believe that you want to say "Large-scale atmospheric and sea ice anomalies observed in CESM historical time series (1850-2005) for the years when ice-core-derived SMB is within highest 10% of the all SMB values in the past ~240 years….."
As explained in the text, CESM is a global climate model, not bound by reanalyses (unlike RACMO2, for example), which generates its own internal climate. This means that the observed SMB time series cannot be directly compared to CESM SMB; instead, we use a statistical approach and select the ten years in the CESM time series with the highest SMB in the 1850-2005.

Figure 9
- Change "accumulation" in the figure to "SMB".
Done
- Change the caption so that it is clearer that this figure shows SMB reconstructed with ice cores over the continent.
Done

Figure S1
- Change to "….sections of sampling for major ions at 10 cm and 5 cm intervals. Isotope samples were taken at 5 cm intervals for the entire core."
Amended, except intervals is replaced by resolution.

- 2 sigma is used in Figure 5 to identify volcanic signals, whereas 4 sigma is used in this figure. I don't really see the merit to see this line; remove this line or justify why not 2 but 4 sigma is used here as a reference.
Removed

- It is impossible to distinguish light and dark gray colors in the ECM plot. And it is more important to show the 301-point (30 cm?) –smoothed ECM values in the figure because the smoothed ECM was used to facilitate annual layer counting.
The light grey line has been removed. The running mean shown here uses a 0.05 m smoothing window on top of the Savitsky Golay 301-point filter.

- I believe that only ECM data are shown in terms of the standard deviation, but not water stable isotopes and major ions (change the caption).
Done

Figure S2
- Add unit "sigma" to the first ECM panel.
Done

Appendix
- Again, use "accumulation" and "SMB" consistently.
Done
- Are latitude/longitude given in decimal degrees?
Yes

Ice core evidence for a 20th century increase in surface mass balance in coastal Dronning Maud Land, East Antarctica

Morgane Philippe[1], Jean-Louis Tison[1], Karen Fjøsne[1], Bryn Hubbard[2], Helle A. Kjær[3], Jan T. M. Lenaerts[4], Reinhard Drews[5], Simon G. Sheldon[3], Kevin De Bondt[6], Philippe Claeys[6], Frank Pattyn[1]

[1]Laboratoire de Glaciologie, Département des Géosciences, Environnement et Société, Université Libre de Bruxelles, BE-1050 Brussels, Belgium
[2]Centre for Glaciology, Department of Geography and Earth Sciences, Aberystwyth University SY23 3DB, United Kingdom
[3]Centre for ice and climate, Niels Bohr Institute, University of Copenhagen, Juliane Maries Vej 30, 2100, Copenhagen, Denmark
[4]Institute for Marine and Atmospheric ~~research~~Research Utrecht, Utrecht University, Princetonplein 5, 3584 CC Utrecht, Netherlands
[5]Bavarian Academy for Sciences and Humanities, Alfons-Goppel-Strasse 11, 80539 Munich, Germany
[6]Department of Analytical Environmental and Geo-Chemistry, Vrije Universiteit Brussel, Pleinlaan 2, BE-1050 Brussels, Belgium

Correspondence to: M. Philippe (mophilip@ulb.ac.be)

Abstract. Ice cores provide temporal records of ~~Surface Mass Balance (SMB), a crucial component of Antarctic~~surface mass balance~~.~~ (SMB). Coastal areas of Antarctica have relatively high and ~~sensitive SMN~~variable SMB, but are under-represented in records spanning more than 100 years. Here we present ~~records~~SMB reconstruction from a 120~~-~~-m-long ice core drilled in 2012 on the Derwael Ice Rise, coastal Dronning Maud Land ~~(DML),~~, East Antarctica~~ in 2012~~. Water stable isotopes ($\delta^{18}O$ and δD) stratigraphy is supplemented by discontinuous major ion profiles and continuous electrical conductivity measurements~~ (ECM).~~. The base of the ice core ~~bottom~~ is dated ~~back~~ to 1759 ± 16 ~~A.D.~~AD, providing a climate proxy for the past ~250 years. The ~~resulting~~core's annual layer thickness history is combined with ~~the~~its gravimetric density profile to reconstruct the site's SMB history, corrected for the influence of ice deformation. The mean ~~long-term SMB~~SMB for the core's entire history is 0.47 ± 0.02 m water equivalent (w.e.) a^{-1}. ~~Reconstructed~~The time-series of reconstructed annual SMB ~~show an~~shows high variability, but a general increase ~~in at least~~~~from~~ beginning in the 20th century. This increase is particularly marked during the last 50 years ~~to a~~(1962 – 2011), which yields mean ~~value~~SMB of 0.61 ± 0.01 m w.e. a^{-1}~~ between 1962 and 2011~~. This trend is compared with other reported SMB data in Antarctica, generally showing a high spatial variability. Output of the fully coupled Community Earth System Model suggests that, although atmospheric circulation is the main factor influencing SMB, variability in sea surface temperatures

and sea ice cover in the precipitation source region also explain part of the variability in SMB~~, along with local~~. Local snow redistribution~~. The latter likely has a significant impact on~~ can also influence interannual variability but ~~not on~~is unlikely to influence long-term trends~~.~~ significantly. This is the first record from a coastal ice core in East Antarctica ~~showing a steady increase of~~to show generally, but not monotonically, increasing SMB ~~during~~over the p~~20th and 21st~~ast two centuries.

1 Introduction

In a changing climate, it is important to know the ~~Surface Mass Balance~~surface mass balance (SMB, i.e. precipitation minus evaporation, sublimation, meltwater runoff, and/or erosion) of Earth's ice sheets as it is an essential component of their total mass balance, directly affecting sea level (Rignot et al., 2011). The average rate of Antarctic contribution to sea level rise is estimated to have increased from 0.08 [–0.10 to 0.27] mm a^{-1} for 1992–2001 to 0.40 [0.20 to 0.61] mm a^{-1} for 2002–2011, mainly due to increasing ice discharge from ~~coastal~~ West Antarctica (Vaughan et al., 2013), ~~-~~where the present-day warming seems to be ~~confined~~focused (Turner et al., 2005; Bromwich et al., 2014; Ludescher et al., 2015).

Some studies suggested that this increase in dynamic ice loss could be partly ~~balanced~~compensated for by a warming-related increase in precipitation (e.g Krinner et al., 2007, Palerme et al., 2016) by the end of the 21st century, but this is subject to debate. For example, Frieler et al. (2015) ~~showed~~argued on the basis of ice core data and modelling that past Antarctic SMB ~~were~~was positively correlated with ~~past~~ air temperature during glacial–interglacial changes~~, using ice core data and modelling.~~. However, Fudge et al. (2016) found that SMB and temperature ~~are~~have not always been positively correlated in West Antarctica.~~ There has been no significant long-term trend in the SMB over the continent during the past few decades (Van de Berg et al., 2006; Monaghan et al., 2006; van den Broeke et al., 2006; Bromwich et al., 2011; Lenaerts et al., 2012; Wang et al., 2016).~~

A clear spatio-temporal pattern in Antarctic SMB change is yet to emerge. Figure 1 and Table A1 summarize results of SMB trends from studies based on ice cores, stake networks and radar. For the continent as a whole, there appears to have been no significant long-term trend in the SMB over the past few decades (Nishio et al., 2002; Van de Berg et al., 2006; Monaghan et al., 2006; van den Broeke et al., 2006; Bromwich et al., 2011; Lenaerts et al., 2012; Wang et al., 2016). Accordingly, 69% of studies show <10 % change over the last ~50 years relative to the last ~200 years. For example, Isaksson et al. (1996) found <3 % change at the EPICA drilling site (Amundsenisen) in Dronning Maud Land, (DML) between 1865-1965 and 1966–1991. Considering studies comparing only the last 20 years with the last 200 years, the percentage reporting no significant trend falls from 69 % to 46 %. The trends revealed over this time period are both negative and positive, although slightly in favour of the latter with 18 % of studies showing a decrease of >10 % and 36 % showing an increase of >10 %. These data compare with 9 % and 21 % respectively of studies reporting SMB change over the past ~50 years. This analysis therefore hints at a recent increase in SMB change, whether positive or negative. Indeed, at some locations SMB change appears only to have begun ~20 years ago (e.g., Site M: Karlof et al., 2005).

Regionally, East Antarctica appears to have experienced recent positive mass balance as a whole (Shepherd et al., 2012) and particularly at inland sites, e.g. at South Pole Station (Mosley and Thompson, 1999), Dome C (Frezzotti et al., 2005), Dome A (Ren et al., 2010; Ding et al., 2011), and DML (Moore et al., 1991; Oerter et al., 2000). However, in DML the picture is by no means clear, with some studies reporting little or no recent SMB change (Isaksson et al., 1999; Oerter et al. 1999, 2000; Hofstede et al., 2004; Fernandoy et al., 2010) and others reporting negative change, both inland (e.g. Anschutz et al., 2011) and near the coast (Kaczmarska et al., 2004: S100; Isaksson and Melvold, 2002: Site H; Isaksson et al., 1999: S20; Isaksson et al., 1996: Site E; Isaksson et al., 1999: Site M). Altnau et al. (2015) compiled DML SMB records and reported a statistically significant positive trend for the region's interior and a negative trend for the coast. In contrast, satellite data and regional climate models indicate a recent increase in precipitation in coastal East Antarctica~~, satellite radar and laser altimetry suggest recent mass gain (Shepherd et al.,~~ (Davis et al., 2005, Lenaerts et al., 2012). ~~Dronning Maud Land (DML) in particular, has~~Similarly, King et al. (2012) estimated on the basis of glacial isostatic adjustment modelling that a 60 ±13 Gt a^{-1} mass increase calculated for the East Antarctic Ice Sheet during the last 20 years was concentrated along its coastal regions, particularly in DML. Indeed, coastal DML appears to have experienced several high SMB years since 2009 (Boening et al., 2012; Lenaerts et al., 2013), similar to positive trends in coastal West Antarctica (Thomas et al., 2008; Aristarain et al., ~~). Calibrated~~2004). Such increases are supported by calibrated regional atmospheric climate ~~model~~ models, which indicate higher SMB ~~during 1980–2004~~ along ~~the~~ coastal sectors during the period 1980–2004 (e.g. Van de Berg et al., 2006~~) and~~). Further, Wang et al. (2016) ~~found~~reported that climate models generally underestimate SMB in coastal DML. This is broadly consistent with the analysis of Frezzotti et al. (2013) who compared sites with low SMB (<0.3 m water equivalent (w.e.) a^{-1}) with sites with high SMB (>0.3 m w.e. a^{-1}), reporting that most of the high SMB sites show an increase in SMB.

It is therefore apparent that, while there is a clear need for data from all of the coastal areas of East Antarctica (ISMASS Committee, 2004; van de Berg et al., 2006; Magand et al, 2007; Wang et al., 2016), Thisthere is particular uncertainty concerning the SMB history of the coastal region is therefore of particular interest.

Ice cores provide temporal records of SMB, which are essential to calibrateof DML. Indeed, although 17 of the records summarized in Table A1 report data from ice cores drilled below 1500 m above sea level and within 100 km of the DML coast, only two of these cover a period longer than 100 years: S100 (Kaczmarska et al., 2004) and B04 (Schlosser and Oerter, 2002), both indicating a small negative trend (Fig. 1, Table A1). Despite this scarcity, SMB records from such cores are valuable for several reasons, including evaluating regional climate models (e.g. Lenaerts et al., 2014), calibrating internal reflection horizons in radio-echo sounding records (e.g. Fujita et al., 2011; Kingslake et al., 2014), to forceand validating ice sheet flow and dating models (e.g. Parennin et al., 2007) and to evaluate regional climate models (e.g. Lenaerts et al., 2014). However, records of SMB are still scarce relative to the size of Antarctica. While the majority show no significant trend in SMB over the last century (e.g. Nishio et al., 2002), some show an increase (e.g. Karlof et al., 2005), and others show a decrease (e.g. Kaczmarska et al., 2004). Frezzotti et al. (2013) compiled SMB records for the whole of Antarctica and 2007). Cores from coastalAltnau et al. (2015) for DML more specifically. Frezzotti et al. (2013) showed no significant SMB changes over most of Antarctica since the 1960s, except for an increase in coastal regions with high SMB and in the highest part of the East Antarctic ice divide. Altnau et al. (2015) found a statistically significant positive trend in SMB for the interior DML and a negative trend at the coast.

However, there is still a clear need for data from the coastal areas of East Antarctica (ISMASS Committee, 2004; van de Berg et al., 2006; Magand et al, 2007; Wang et al., 2016), where few studies focused on ice cores spanning more than 100 years. Coastal regions allow also generally provide higher temporal resolution than from the interior asbecause SMB generally decreasedecreases with both elevation and distance from the coast (Frezzotti et al., 2005). IceNear the coast, ice rises arerepresent ideal locations for paleoclimate studies (Matsuoka et al., 2015) asbecause they are undisturbed by up-stream topography, and lateral flow is almost negligible. Melt, and melt events are also likely to be much less frequent than on ice shelves (Hubbard et al., 2013).

In this paper we report on water stable isotopesisotope (δ^{18}O and δD) measurements (5–10 cm resolution)), major ion and continuous electrical conductivity measurement (ECM) data along a 120 m-long ice core drilled on the Derwael Ice Rise (DIR) in coastal DML. This record is complemented by major ion and continuous electrical conductivity measurement (ECM) profiles to improve the resolution of the seasonal cycles wherever necessary.We date the core base to 1759 ± 16 AD by layer-counting. After correcting for dynamic vertical thinning, we derive annual SMB, and calculate average SMB and trends overannual SMB for the last 254 ± 16~250 years, i.e. across the Anthropocene transition. These are compared , and compare them with other reported trends in Antarctica, including DML, over the last decades. from the region.

2 Field site and methods

2.1 Field site

The study site is located in coastal DML, East Antarctica. A 120 m-long ice core, named IC12 after the project name IceCon, was drilled in 2012 on the dividecrest of the DIR–, which is 550 m thick (70°14’44.88’’S, 26°20’5.64’’E, 450 m a.s.l., Fig. 1). This ice rise is 550 m thick and the recent SMB has been estimated to 0.50 m w.e. a^{-1} from preliminary ice core analysis (Drews et al., 2015; Callens et al., 2016). 1).

Ice rises provide scientifically valuable drill sites because they are located close to the ocean (and hence sample coastal precipitation regimes) and because ground-penetrating radar data can easily identify drill sites on a local dome that are relatively undisturbed by horizontal flow. However, a number of regional factors complicate the interpretation of ice-core records on ice rises: ice rises form topographic barriers with the capacity to disrupt atmospheric circulation on otherwise flat ice shelves. Orographic precipitation can thereby result in significantly high SMB values on the upwind sides of such ice rises, with corresponding precipitation shadows on the downwind side (Lenaerts et al, 2014). For the DIR in particular, the SMB on the upwind side is up to 2.5 times higher than on the downwind side (Callens et al., 2016). On top of this larger scale (~10 km) asymmetry, Drews et al. (2015) identified a small scale (km) SMB oscillation near the dividecrest, tentatively attributed to erosion at the crest, and subsequent redeposition on its downwind side. The observedRadar stratigraphy shows that the local SMB maximum is therefore offset bylocated ~4 km from the topographic divide whereupwind of the ice core was drilleddrill site. This means that the absolute values of the ice-core derived SMB sample a regime where the SMB varies on short spatial scales. Moreover, Drews et al. (2015) identified isochrone arches (a.k.a. Raymond Bumps) beneath the divide. This characteristic flow pattern causes ice at shallow to intermediate depths beneath the divide to be older than at comparable depths in the ice-rise flanks, necessitating a specific strain correction for the ice-core analysis, which we discuss below. Both Drews et al. (2015) and Callens et al. (2016) suggested that the DIR has maintained its local ice dividecrest for the last thousands of years and possibly longer. By matching the radar stratigraphy to an ice-flow model, Drews et al. (2015) suggested that the DIR dividecrest elevation is close to steady-state and has potentially undergone modest surface lowering in the past. Both studies used a temporally constant SMB. Here we focus on the temporal variability and argue that, because the DIR has been stable in the past, we can draw conclusion with respect to the larger-scale atmospheric circulation patterns.

2.2 Ice coring and density analyses

The IC12 ice core was drilled with an Eclipse electromechanical ice corer in a dry borehole. The mean length of the core sections recovered after each run was 0.77 m and the standard deviation 0.40 m. The ice core is complete, except for the 100-101 m section, which fell back in the borehole and was recovered in broken pieces. Immediately after drilling, temperature (Testo 720 probe, inserted in a 4 mm~~-~~-diameter hole drilled to the centre of the core, precision ±0.1 °C) and length were measured on each core section, which was then wrapped in a PVC bag, stored directly in a refrigerated container at -25 °C, and kept at this temperature until analysis at the home laboratory. ~~The~~Here, core sections were ~~then~~ bisected lengthwise~~,~~ in a cold room at -20 °C. One half of the core section was used for ECM measurements and then kept as archive, and the other half was sectioned for water stable isotope sampling and major ion analysis. Only a few very thin (1 mm) ice layers are present in the core. A best-fit through discrete gravimetric density measurements, previously published (Hubbard et al., 2013), is used here to convert measured annual layer thicknesses to ~~meters water equivalent (w.e.)~~m w.e. (Sect. 2.3).

2.3 Annual layer counting and dating

2.3.1 Water stable isotopes and major ~~ion~~ions

Half of each core section was resampled as a central bar of 30 mm x 30 mm square section with a clean band saw. The outer part of the half-core was melted and stored in 4 ml bottles for subsequent $\delta^{18}O$ and δD ~~measurements~~analysis, completely filled to prevent contact with air. For major ion measurements, the inner bar was placed in a Teflon holder and further decontaminated by removing ~2 mm from each face under a class-100 laminar flow hood, using a methanol-cleaned microtome blade. Each 5 cm~~-~~-long decontaminated section was then covered with a clean PE storage bottle, and the sample cut loose from the bar by striking it perpendicular to the bar axis. Blank ice samples prepared from milliQ water were processed before every new core section and analysed for contamination.

Dating was achieved by annual layer counting identified from the stratigraphy of the $\delta^{18}O$ and δD isotopic composition of H_2O measured with a PICARRO L 2130-i Cavity Ring Down Spectrometer (CRDS) (precision, $\sigma = 0.05$ ‰ for $\delta^{18}O$ and 0.3 ‰ for δD). This composition was generally measured at 10 cm resolution in the top 80 m and 5 cm resolution below (See Fig. S1 for exact resolution). For sections of unclear isotopic seasonality, major ion analysis (Na^+, Cl^-, $SO_4^=$, NO_3^- and methylsuflonic acid (MSA)) was additionally carried out using a Dionex-ICS5000 liquid chromatograph, at 5 cm resolution. The system has a standard deviation of 2 ppb for Na^+ and $SO_4^=$, 8 ppb for Cl^-, 7 ppb for NO_3^-, and 1 ppb for MSA. Non sea-salt sulfate was calculated as $nssSO_4=[SO_4^=]_{tot} - 0.052*[Cl^-]$, following Mulvaney et al. (1992) and represents all $SO_4^=$ not of a marine aerosol origin. The ratio $Na^+/SO_4^=$ was also calculated as an indicator of seasonal $SO_4^=$ production.

2.3.2 ECM measurements

ECM measurements were carried out in a cold room at -18°C at the Centre for Ice and Climate, Niels Bohr Institute, University of Copenhagen, with a modified version of the Copenhagen ECM described by Hammer (1980). Direct current (1250 V) was applied at the surface of the freshly-cut ice and electrical conductivity was measured at 1 mm resolution. The DC electrical conductivity of the ice, once corrected for temperature, depends principally on its acidity (Hammer, 1980; Hammer et al., 1994). This content varies seasonally and usually shows longer term localized maxima associated with sulfate production from volcanic eruptions. ECM can therefore be used both as a relative and an absolute dating tool.

As measurements were principally made in firn, we applied ~~a novel~~the technique described by Kjær et al. (~~in review~~2016) to correct for the effect of ~~the~~ firn porosity on the amplitude of the signal. ~~As the~~Because ECM ~~current is low for higher~~scales inversely with air content, we multiplied the ~~high resolution~~measured ECM signal by ~~the inverse of the ice volume fraction, i.e.~~ the ratio of the ice density to firn density (ρ_{ice}/ρ_{firn}), using the gravimetric density best fit from Hubbard et al. ~~(2013).~~
~~ECM data were~~(2013). While there are millimetric-scale differences between the optical televiewer log and the ice core depth scales used to derive this best-fit, the correlation provides an acceptably high coefficient of determination ($R^2 = 0.96$) for this purpose. ECM data were then smoothed with a 301 point first-order Savitsky–Golay filter (Savitsky and Golay, 1964) which eliminates peaks due to random noise and small-scale variations in material chemical composition while preserving the larger peaks, including those due to volcanic eruptions. Finally, the ECM data were normalized by substracting the mean and dividing by the standard deviation following Karlof et al. (2000).

2.4. Corrections for ice flow

The compression of snow under its own weight not only involves vertical density changes ~~along the vertical~~, but also involves lateral deformation of the underlying ice. Failure to take the latter process into account would provide an underestimation of reconstructed initial annual layer thickness, and therefore of the SMB, especially within the deepest and hence oldest part of the record. In this paper,We explore two different models are used to represent vertical strain rate evolution with depth: (i) strain rates derived from a full Stokes model that represent the full Raymond effect measured at the ice divide (Drews et al., 2015); and (ii) a modified Dansgaard–Johnsen model (Dansgaard and Johnsen, 1969) based on the description given in Cuffey and Paterson (2010).

The Drews et al. (2015) strain rate profile accounts for the best fit with theto radar layers at depth, taking into account a small amount of surface thinninglowering (0.03 m a^{-1}) and rheological anisotropy (althoughof the ice (run A(n=3), dH = 100, chi = 0.03 m/a, layer-depth SMB). The magnitude of applied surface lowering is small and does not alter the former is not essential). From a hexagonal strain network, we calculated strain rates significantly compared to a steady-state scenario. To determine horizontal strain rates independently, we used data from 8 markers located along a circle with a 2 km radius around the dome. The markers were positioned using differential GPS in 2012 and 2013 (Drews et al., 2015). The horizontal strain rates ($\varepsilon_{xx} + \varepsilon_{yy}$) were calculated to be 0.0022 x 10^{-3} a^{-1}. Mass conservation then gives a vertical strain rate at the surface of -0.0022 x 10^{-3} a^{-1}. The shape of the vertical velocity profile was then used and scaled to match this measured value. A best fit to the measured radar layers was obtained with a value of a mean SMBthe long-term accumulation rateSMB of 0.55 m a^{-1} ice equivalent (Fig. 2).

Alternatively, we used the The second model, based on Dansgaard–Johnsen (D–J) model), was used to fit the characteristics of the Raymond effect at the ice divide, exhibited by the Raymond effect.. Assuming that the horizontal velocity here is zero, the vertical velocity is maximum at the surface and equals, given by the SMB (with negative sign)), and is zero at the bed. Assuming a vertical strain rate of -0.002 a^{-1} at the surface, we can determine the kink point (between constant strain rate above and a strain rate linearly decreasing with depth below) that obeys these conditions (Cuffey and Paterson, 2010). This approach indicates that the kink point lies at 0.9H, where H is the ice thickness. As seen in Fig. 2b, this method yields a vertical strain pattern that is consistent with that of Drews et al. (2015), especially in the first 120 m corresponding to the length of the ice core.

We Both strain rates (Drews/D–J) were then used to correct the ice equivalentcalculate annual layer thickness for strain thinning., and consequent SMB, using vertical strain rates determined by both the Drews and the D–J methods. Annual layer thicknesses were then converted from ice equivalent to w.e. for easierto facilitate comparison with other studies.

2.5 Community Earth System Model (CESM)

Atmospheric reanalyses (ERA-Interim, Dee et al., 2009) and regional climate models are compared to the ice core SMB in Sect. 3.4.. These models extend back to 1979, ~~which means that they cover~~covering only a small proportion of the ice core record. ~~Instead~~Thus, to interpret our ice~~-~~-core~~-~~-derived SMB record and relate it to ~~the~~ large-scale climate conditions, we use SMB, sea ice and temperature output from the Community Earth System Model (CESM). CESM is a global, fully coupled, CMIP6-generation climate model with an approximate horizontal resolution of 1°, and has recently been used successfully to simulate present-day Antarctic climate and SMB (Lenaerts et al., 2016). ~~We~~Because CESM is not bound by observations, and is a freely evolving model that generates its own climate, the simulated SMB time series cannot be directly compared to the observed one. Instead we use a statistical approach: we use the historical time series of CESM (156 years, 1850–2005) that overlaps with most of the ice core record, and group the 16 single years (i.e. ~10 %)~~-~~ with the highest SMB and lowest SMB in that time series. We take the mean SMB of the ice covered CESM grid points of the coastal region around the ice core (20–30 °E, 69–72 °S) as a representative value. For the grouped years of highest and lowest SMB, we take the anomalies (relative to the 1850–2005 mean) in near-surface temperature and sea-ice fraction as parameters to describe the regional ocean and atmosphere conditions corresponding to these extreme years. The ~~CESM simulated~~ sea-ice extent ~~in~~simulated by CESM during the observational period ~~is very realistic compared to~~matches observations closely (Lenaerts et al., 2016) and does not show any temporal trend in the Atlantic sector, ~~which gives us~~providing confidence that the model treats sea ice ~~is treated~~ realistically.

3 Results

3.1 Dating

3.1.1 Relative dating (seasonal peak counting)

~~Figures 3, S1 and S2 illustrate how the~~Annual layers are identified on the basis of high-resolution water stable isotopes ($\delta^{18}O$, δD), smoothed ECM, chemical species and their ratios ~~are used in combination to identify annual layer boundaries. All~~(Figs. 3, S1 and S2). While all of these physico-chemical ~~variables~~properties generally show a clear seasonality, ~~undisturbed by~~ they also change smoothly over the few very thin ice layers identified in the core (white dots in Fig. ~~3).~~3), indicating that they are not disturbed by surface melting. The summer peak in water stable isotopes is obvious in most cases. The boundary between annual layers was identified as the middle depth of the peak above the mean $\delta^{18}O$ value (thin black line in Fig. 3), considered as the “summer season”. Major ionions such as $nssSO_4$, NO_3^-, and especially the ratio $Na^+/SO_4^{=}$, generally help to distinguish ambiguous peaks in the isotopic record. $SO_4^{=}$ is one of the oxidation products of Dimethyl Sulfide (DMS), a degradation product of DMSP (dimethylsulfoniopropionate) which is synthesized by sea ice microorganisms (sympagic) as an antifreeze and osmotic regulator (e.g. Levasseur, 2013). Both $nssSO_4$ and $Na^+/SO_4^{=}$ vary seasonally. NO_3^- also shows a seasonal signal, but the processes controlling its seasonality are not yet fully understood (Wolff et al., 2008). For ECM, there is also a regular seasonal signal, which is sometimes blurred below 80 m, although some seasonal cycles can still be seen, for example between 115 and 118 m. (Fig. S2). Two extreme age–depth profiles (youngest and oldest) resulted from this counting procedure, taking the remaining ambiguities into account (Fig. S2). The mean age–depth profile is presented in Fig. 4 with the ranges associated with the two extreme age–depth estimates. Between 237 and 269 annual cycles were identified between the reference surface (November 2012 A.D.)AD) and the bottom of the core, which is consequentlycorrespondingly dated to 1775 AD and 1743 AD respectively, with a mean age of 1759 ± 16 A.D..AD.

In the oldest estimate, each $Na^+/SO_4^{=}$ can generally be associated with a trough in $\delta^{18}O$ minimum, even in the deep parts of the record. This is the case between 101 and 110 m or between 112 and 115 m, for example (Fig. S2), while in the youngest estimate, these years show a double peak in $Na^+/SO_4^{=}$, suggesting the latter underestimates the number of years. We will now see if we can find a confirmation for trusting this oldest estimate fromThis age-depth range may be evaluated further on the basis of identifying volcanic signals in the core's ECM record.

3.1.2 Can we identifyRefinement of the age-depth scale on the basis of volcanic horizons to refine our depth-age scale?

Volcanic indicators (ECM, $nssSO_4$, $SO_4^{=}/Na^+$) can potentially be used to identify specific, dated volcanic eruptions, allowing us to reduce the uncertainties resulting from the relative dating procedure. However, the unambiguous eruption identifications areidentification of eruptions is challenging in ice cores from coastal regions, where the ECM and $nssSO_4$ background signals are commonly highly variable due to the proximity of the ocean and ocean-related MSA products (Fig. S1). Given our preliminary relative core-based date of 1759 ± 16 AD (Section 3.1.1 above), we searched our ECM record for volcanic horizons of known ages that fell within our relative age range. The best match here is provided by our oldest age-depth scale, with the major Tambora eruption seeming to appear at 102.35 m (Fig. 5). Here, the peak in our ECM record exceeds 4σ, while an adjacent earlier peak, exceeding 2σ, may be attributed to an eruption from an unknown volcano in 1809 (Traufetter et al., 2004). Although these ECM responses are less pronounced than in other inland cores such as at WAIS divide (Sigl et al., 2013), a 2σ threshold is commonly considered as sufficient evidence for a match to volcanic eruptions (e.g. Kaczmarska et al., 2004) and allows potential matching of 13 volcanoesS1). within our record. However, several other peaks above 2σ could not be associated with any known volcanic eruption. Given this uncertainty, we conclude that the core's ECM record is too noisy for our age-depth scale to be refined with confidence by matching to volcanic eruptions. We therefore keep both estimates resulting from our layer-count-based dating process and use them as an indication of the influence of dating uncertainty on our SMB reconstruction.

Given the preliminary dating of 1759 ± 16 A.D. made on the basis of our relative core dating (Section 3.1.1 above), we have looked for volcanic horizons at the depths corresponding to the oldest estimate to try and refine this timescale (Figure 5). The Tambora eruption seems to appear at 102.35 m, with an ECM signature above the 4σ threshold and a consecutive peak above the 2σ threshold, which could be attributed to the 1809 eruption (unknown volcano, Traufetter et al., 2004). Although this is much less pronounced than in other cores, more inland, such as WAIS divide (Sigl et al., 2013), this threshold is usually considered as sufficient (e.g. Kaczmarska et al., 2004) and allows potential matching of 13 volcanoes. However, many other peaks above that threshold could not be associated with any known volcanic eruption. Therefore, we concluded that the background is too noisy to refine the relative time scale in this core. As a result, we will keep both estimates resulting from our relative dating process as an evaluation of the influence of the dating uncertainty on our SMB reconstruction.

3.2 Surface Mass Balancemass balance record

Combining the annual layer thickness data set with the gravimetric density best fit (published in Hubbard et al., 2013),2013) and thinning rate corrections, we reconstructed the SMB record at the DIR summit of the DIR from 17441759 ± 16 years AD to 2011.November 2012 (Fig. 6). Without correction for layer thinning, the mean annual layer thickness is 0.36 ± 0.02 m w.e.. This is compared with

We applied two corrections: the modified Dansgaard–Johnsen model and the adapted full Stokes model (Drews et al., 2015) (see Sect. 4.2) to investigate the influence of ice deformation on annual layer thicknesses, assuming a constant SMB.

Figure 6a shows the reconstructed history of annual layer thicknesses at IC12 from 1744 to 2011, without ice deformation and with the two different ice-deformation models (modified D-record of SMB including corrections for thinning, via Drews and D-J model and Drews et al., 2015), which overlie each other at this scale. From now on, we will only consider (Sect. 2.4 above) in Fig. 6a. Both corrections are undistinguishable. Since the correction ofbased on Drews et al. (2015) as it is both similar to the modified D-J model and more closely guided by field measurements. As expected, annual layer thicknesses without ice deformation are underestimated in the oldest part of the ice core relative to that with ice deformation taken into account. Figure 6 (b–d) shows both than the modified D-J model we henceforth consider only the record corrected by Drews. Figures 6b and 6c show the oldest and the youngest estimates to evaluate the influence of the dating uncertainty. The mean annual SMB, i.e., the mean corrected annual layer thickness, is 0.47 ± 0.02 m w.e.a^{-1}. Asrespectively and include an 11-year running mean applied to reduce interannual variability is high, the 11 year running means. Error bars are also shown. All curves derived from the 5 – 10 cm depth uncertainty on annual layer thickness, depending on the water stable isotopes resolution and converted to m w.e.. The uncertainty range drawn in Fig. 6d is bounded by the oldest and youngest estimates. The mean SMB for the whole period is 0.47 ± 0.02 m w.e., ranging between 0.26 ± 0.01 m w.e. and 1 ± 0.03 m w.e.. All curves also show a clear positive trend in SMB from at least the second half of the 20th century.

Table 1 shows average SMB for three

We define four different SMB time periods (chosen mainly for summarized in Table 1) beginning from 1816 because of the Tambora marker (allowing comparison with previousother studies) starting from the Tambora eruption (1816–2011):, Table A1) and because confidence is reduced by the decreasing signal to noise ratio before this. 2012 is not included in these summaries as it does not cover a full year. These periods are: (i) the full 195 year time period (1816 to 2011) (ii) the last 111 years comparedrelative to the previous full time period of time (i.e.., 1900–2011 cf. 1816–1900), (iii) the last 50 years comparedrelative to the previous full time period of time (i.e., 1962–2011 cf. 1816–1961), and (iv) the last 20 years comparedrelative to the previous full time period of time (i.e.., 1992–2011 cf. 1816–1992). From For the full 195 year time period (1816 to 2011,), the averagemean SMB, including correction for layer thinning, is 0.49 ± 0.02 m w.e. a^{-1}. For the last 111 years, (1900–2011), the SMB is 0.55 ± 0.02 m w.e. a^{-1}, representing a 26 ± 1 % increase compared to the previous period. For the last 50 years (1962–2011), the SMB is 0.61 ± 0.01 m w.e. a^{-1}, representing a 32 ± 4 % increase compared to the previous period. For the last 20 years (1992–2011), the SMB is 0.64 ± 0.01 m w.e. a^{-1} and the, representing a 32 ± 3 % increase compared to the previous period is 32 ± 3 %. .

Table 2 shows the detailedDetailed annual SMBSMBs reconstructed for the last 10 years for our oldest and youngest estimates. In are summarized in Table 2. These records indicate recent SMB values that fall at the top end of those reconstructed throughout the period 1816-2011. For the oldest estimate, the highest SMB during the last 10 years occurred in 2011 and , followed by 2009, which belong to the . With values of 0.98 m w.e. a^{-1} % and 30.82 m w.e. a^{-1}, these fall within the 1 % and 2 % highest SMB years of the whole record, (~250 years) respectively. InFor the youngest estimate, the highest SMB during the last 10 years occurred in 2011, followed closely by 2002 is higher thanand 2009. With values of 0.98 m w.e. a^{-1}, 0.89 m w.e. a^{-1}, and 0.82 m w.e. a^{-1}, these fall within the 1 %, 2 % and 3 % highest SMB years of the whole record respectively.

3.3 Sources of uncertaintiesuncertainty

Surface Mass Balancemass balance reconstructed from ice cores can be characterized by substantial uncertainty (Rupper et al., 2015). The accuracy of reconstructed SMB depends on the dating accuracy, which, in our case, is determinedbounded by the oldest and youngest estimates. Also, given our vertical sampling resolution of $\delta^{18}O$, the location of summer peaks is only identifiable to a precision of 0.05 m where no other data are available, but this error only affects SMB at an . However, our multi-parameter records (Figs 3 and S1) indicate that annual resolution, as shown by error-bars in Fig. 6. Note also that itlayer thickness throughout the core's full length (and particularly since ~1815, the time period we focus on) is very unlikelygreater than our sample length, providing confidence that we have overestimated the number of years due to the are not missing annual layers that are thinner than our samples. Our belief that $\delta^{18}O$ sampling resolution, since a cycles demarcate annual layers throughout the record is further supported by the one-to-one correspondence subsists,between this parameter and the $Na^+/SO_4^=$ ratio, even in the deepest part of the core, between the $\delta^{18}O$ and the $Na^+/SO_4^=$ ratio.

SMB reconstructions are also influenced by density measurement error ((~2 % errorherein) and small-scale variability in densification. TheHowever, the influence of this effect on SMB is very small. For example, Callens et al. (2016) for example, used a semi-empirical model of firn compaction (Arthern et al., 2010) adjusting its parameters to fit the discrete measurements instead of using the best fit from Hubbard et al. (2013). UsingApplying the first model changesof Callens et al. (2016) to our data results in reconstructed SMB mean values that differ by less than 2 %.% from our analysis based on Hubbard et al. (2013).

Average SMB on longer time periods are in all cases more robust than reconstructed annual SMB because they are less affected by uncertainties. These average estimates are also useful to reduce the influence of inter-annual variability.

Vertical strain rates also represent a potential source of error. A companion paper (Philippe et al., in prep.) will be dedicated to a more precise assessment of this factor using repeated borehole optical televiewer stratigraphy. However, the present study uses a field-validated strain rate model which is as close as possible to reality, and shows that using the simpler modified Dansgaard–Johnsen model changes the reconstructed SMB by maximum 0.001 m w.e. a^{-1}. Therefore, we are confident that refining the strain rate profile will not change our main conclusions.

~~Another possible source of error is the potential migration of the ice divide. Indeed, radar layers show SMB asymmetry next to the DIR divide. However, Drews et al (2015) found that the ice divide of the DlR must have remained laterally stable for thousands of years to explain the comparatively large Raymond arches in the ice stratigraphy. Callens et al. (2016) find a similar argument by using the radar stratigraphy in the ice-rise flanks. The possibility for an ice-divide migration is therefore small.~~

Temporal variability of SMB at certain locations can also be due to the presence of surface undulations upstream (e.g. Kaspari et al, 2004), but this effect is minimised at ice divides.

Another possible source of error is the potential migration of the crest. Indeed, radar layers show SMB asymmetry next to the DIR crest. Although the crest of DIR must have remained laterally stable for thousands of years or more to explain the comparatively large Raymond arches in the ice stratigraphy (Drews et al., 2013; Callens et al., 2016), we cannot exclude a recent crest migration over the last decades, particularly because the lateral offset of the SMB maximum towards the upwind side (inferred from the radar stratigraphy) remains unexplained. However, there is twofold evidence to argue against a recent divide migration (1) ~~because~~ a similar offset in the SMB maximum is also found on another ice rise (Drews et al., 2013), suggesting ~~it is likely~~ that this offset reflects a generic pattern of atmospheric deposition near the crests rather than a recent and coincidental crest migration of two ice divides ~~(Drews et al., 2015).~~and (2) the shallow arches in the radar stratigraphy which define the lateral offset are vertically aligned and not tilted as would be expected for a migrating divide (Drews et al., 2015; Fig. 3b).

3.4 Comparison with climate models

~~Figure 7 compares~~We compare the trend in our IC12 SMB record with outputs from ~~two~~three atmospheric models: ERA-Interim reanalysis (Dee et al., 2009~~) and~~), the CESM model~~.~~ (Fig. 7) and RACMO2 (Lenaerts et al., 2014). ERA-Interim shows no trend in the relatively short overlapping period (1979–2012~~) it covers.~~). The ice core derived SMB correlates moderately to ERA-Interim and RACMO2~~ (Lenaerts et al., 2014),~~, yielding coefficients of determination (R~~^{2} =~~^{2}) of 0.36 and 0.5 respectively. For a longer ~~overlapping~~ period of overlap, we used the output of the CESM model, although it is a freely evolving model that does not allow a direct comparison with measured data. The CESM-derived average SMB at ~~Derwael in CESM (~~the closest grid point~~)~~ to DIR is too low (0.295 ± 0.061 m a^{-1}~~)~~, 1850–2005), probably because the orographic precipitation effect is not well simulated. However, CESM does reproduce ~~(much of)~~ the ~~observed~~general trend reconstructed from our DIR core. Subtle small-scale variations in wind speed and direction, typically not resolved by reanalyses or regional climate models, might disrupt the inter-annual variability of SMB, although we assume that it does not influence the positive SMB trend found in the ice core record. Unfortunately, our method does not allow for an explicit partitioning of the SMB explained by precipitation as opposed to wind processes. Instead, we focus on the drivers of precipitation at the ice core site using the output of CESM (Fig. 8).

In anomalously high SMB years, sea ice coverage is substantially lower than average (20–40 fewer days with sea-ice cover, ~~fig.~~i.e. about 10-30% reduction compared to the average of 120–200 days (Fig. 8) in the Southern Ocean northeast of the ice core location, which is the prevalent source region of atmospheric moisture for DIR (Lenaerts et al., 2013). This is associated with considerably higher near-surface temperatures (1–3 ~~K~~°C). In low-SMB years (not shown~~),~~) we see a reverse, but less pronounced, signal~~,~~ with a higher sea ice fraction (10–20 days~~),~~) and slightly lower temperatures at the oceanic source region of precipitation.

4 Discussion

4.1 Regional-scale variability

Output of the CESM ~~show~~shows that, along with atmospheric circulation, sea-ice cover and near-surface temperatures have an influence on precipitation at a regional scale (Fig. 8).

Orography can also greatly affect SMB variability (Lenaerts et al., 2014~~). Local~~), as can local variations in wind ~~phenomena are important factors of interannual~~strength and ~~spatial variability.~~direction. Indeed, the lower correlation ~~with~~ between SMB derived from ERA-Interim and RACMO2 ~~in~~ and the results of our study~~, as compared to~~ than with those from ice cores collected ~~on~~in West Antarctica (e.g., Medley et al., 2013; Thomas et al., 2015) ~~is presumably~~may be explained by the strong influence of local wind-induced snow redistribution and sublimation ~~on the SMB~~ on the wind-exposed ridge of the DIR (Lenaerts et al., 2014). However, both Drews et al. (2015) and Callens et al. (2016) showed that this spatial SMB pattern has been constant for the last thousands of years. Therefore, our observed trend of increasing annual SMB in the ice core represents the temporal changes and is highly unlikely to be explained by a different orographic precipitation pattern caused by a change in local wind direction or strength.

This argument, along with ~~the existing~~positive correlations with ERA-Interim and RACMO2 outputs, suggests that the ~~observed~~ trend ~~is not limited to the~~we reconstruct at DIR ~~but that it~~ is representative of at least the Roi Baudouin ice shelf, surrounding the DIR. More studies are needed in the area to confirm this inference.

4.2 Continental-scale variability

Our results show ~~an increase in~~ generally increasing SMB on the DIR in coastal DML ~~during~~over the ~~20th and 21st centuries.~~past ~100 years. This ~~confirms studies that show a recent increase in precipitation in coastal East Antarctica on~~trend continues, and possibly accelerates, up to the ~~basis of satellite data~~present. This finding is consistent with the results of large-scale modelling and ~~regional~~ climate ~~models (Davis et al., 2005, Lenaerts et al., 2012). Using a new glacial isostatic adjustment model, King et al. (2012) estimated that a 60 ±13 Gt a^{-1} mass increase for the East Antarctic Ice Sheet during~~ -based studies that also indicate a SMB increase in the ~~last 20 years was concentrated along coastal regions, particularly in DML.~~area (summarized in Section 1 above). However, until now, no increase ~~had~~has been detected in ice cores from the area. Our study is the first to detect in situ an increase in coastal Antarctic precipitation, which is expected to occur mainly in the peripheral areas at surface elevations below 2250 m (Krinner et al., 2007; Genthon et al., 2009).

~~However, not all of Antarctica would be expected to have the same SMB trend. Figure 1 and Table A1 summarize results on SMB trends from previous studies based on ice cores, extended with a few studies based on stake networks and radar. The colours of the sites indicated on Fig. 1 show the SMB change at that site. The reference period corresponds to the last ~200 years, and it is compared to two recent periods of different lengths, corresponding approximately to the last ~50 years and to the last ~20 years. The exact periods are given in Table A1.~~

~~The ISMASS Committee (2004) pointed out the importance of analysing coastal records. Twenty-three of the temporal records found in the literature concern ice cores drilled less than 100 km from the coast and below 1500 m above sea level, among which 17 are located in DML. However, only two of those records cover a period longer than 100 years: S100 (Kaczmarska et al., 2004) and B04 (Schlosser and Oerter, 2002). They both show a small negative trend (Fig. 1).~~

~~For the whole continent, most studies (69 % of those comparing the last ~50 years with the last ~200 years) show no significant trend (< 10 % change).~~Figure ~~For example, Isaksson et al. (1996) found <3 % change at the EPICA drilling site (Amundsenisen, DML) between 1865-1965 and 1966–1991. No trend was found on most inland and coastal sites (e.g. B31, S20) in DML for the second part of the 20th century (Isaksson et al., 1999; Oerter et al. 1999, 2000; Hofstede et al., 2004; Fernandoy et al., 2010). When we consider only the studies comparing the last 20 years to the last 200 years, the percentage reporting no significant trend falls from 69 % to 46 %. The trends revealed are both positive and negative and concern the whole Antarctic continent.~~

A few studies show a decrease of more than 10 % (9 % of the studies observed this decrease during the last ~50 years and 18 % during the last ~20 years). This is the case for several inland sites in DML (e.g. Anschutz et al., 2011), but also coastal sites in this region (Kaczmarska et al., 2004: S100; Isaksson and Melvold, 2002: Site H; Isaksson et al., 1999: S20; Isaksson et al., 1996: Site E; Isaksson et al., 1999: Site M).

Twenty-one percent of the studies record an increase of >10 % of SMB starting during the last ~50 years and 36 % of the studies show such an increase starting during the last ~20 years. In East Antarctica, positive trends were only recorded at inland sites, e.g. in DML (Moore et al., 1991; Oerter et al., 2000), at South Pole Station (Mosley and Thompson, 1999), Dome C (Frezzotti et al., 2005), and around Dome A (Ren et al., 2010; Ding et al., 2011). Other positive trends were found on the Antarctic Peninsula in coastal West Antarctica (Thomas et al., 2008; Aristarain et al., 2004). For some sites, the increase only started ~20 years ago (Site M: Karlof et al., 2005).

Frezzotti et al. (2013) compared the sites with low SMB (< 0.3 m w.e. a^{-1}) with the sites with higher SMB and found that most of the high SMB sites show an increase in SMB. However, Fig. Figure 9 shows that coastal sites (below 1500 m a.s.l. and less than 100 km from the ice shelf) do not all behave similarly. Most of the sites with high accumulation SMB (coastal or not) show an increase in SMB between the last ~50 years and the reference period (last ~200 years), whereas the sites with lower SMB show no trend, even if they are coastal (Fig. 9a). This figure also shows that only two other coastal sites can be used to compare the last ~200 years with the last 20 years (Gomez and S100, Fig. 9b and Table A1). Comparing the last ~20 years with the last ~50 years, the increase is less importantvisible (Fig. 9c).

4.3 Causes of spatial and temporal SMB variability

The positive temporal trendtrends and contrasts in SMB measured here and in ice cores from other areas, as well as the apparent spatial contrast, could be the result offrom thermodynamic forcing (temperature change), dynamic forcing (change in atmospheric circulation) or both.

Higher temperature induces higher saturation vaporvapour pressure, generally enhancing precipitation. Oerter et al. (2000) demonstrated a correlation between temperature and SMB in DML. On longer timescales (glacial–interglacial), using ice cores and models, Frieler et al., (2015) found a correlation between temperature and SMB for the whole Antarctic continent. However, both Altnau et al. (2015) and Fudge et al. (2016) found that SMB and changes in ice $\delta^{18}O$ are not always correlated. They hypothesized that changes in synoptic circulation (cyclonic activity) have more influence than thermodynamics, especially at the coast.

In the presence of a blocking anticyclone at subpolar latitudes, an amplified Rossby wave invokesinduces the advection of moist air (Schlosser et al., 2010; Frezzotti et al., 2013). On these rare occasions, meridional moisture transport towards the interior ~~in~~of DML is concentrated into atmospheric rivers. Two recent manifestations of these short-lived events, in 2009 and 2011, have led to a recent positive mass balance of the East Antarctic ice sheet (Shepherd et al., 2012; Boening et al., 2012). ~~It~~The effect was also ~~observed~~recorded in situ, at a local scale, next to the Belgian Princess Elisabeth base (72 °S, 21 °E) (Gorodetskaya et al., 2013; 2014). Several of these precipitation events in a single year can represent up to 50 % of the annual SMB away from the coast (Schlosser et al., 2010; Lenaerts et al., 2013). At the coast, precipitation is usually event-type, but the events occur ~~during~~throughout the whole year. However, the 2009 and 2011 events are also observed in our data as two notably higher~~-~~-than~~-~~-average SMB years (~~2009 and 2011,~~ Table 2). Our record places these extreme events within a historical perspective. Despite the fact that higher SMB years exist in the recent part of record, 2009 and 2011 are amongst the 2-3 % ~~and 1 %~~ highest SMB years of the last two centuries~~, respectively.~~ for 2009, depending on the estimate, and 1 % for 2011.

A change in climate modes could also partly explain recent changes in SMB. The Southern Annular Mode (SAM) has shifted to a more positive phase during the last 50 years (Marshall, 2003). This has led to ~~increasing~~increased cyclonic activity, but also ~~increasing~~to increased wind speed and sublimation. Kaspari et al. (2004) also established a link between periods of increased SMB and sustained El Niño events (negative Southern Oscillation Index (SOI) anomalies) in ~~1991–95 and 1940–42. In our detrended dataset (not shown), mean SMB is indeed 5 % higher during 1991–95 than the long-term average and 17 % higher during 1940–42. However, high SMB is also recorded during 1973–75 (19 % higher than average) while that period is characterized by positive SOI values. Therefore, climate modes seem to have little influence (or an influence of unconstrained complexity) on inter-annual variability of SMB at IC12.~~ 1940–42 and 1991–95 but our record does not support this observation.

Wind ablation represents one of the largest sources of uncertainty in modelling SMB~~. This~~, and is an important ~~factor generating~~cause of spatial and interannual variability. Highest snowfall and highest trends in predicted snowfall are expected in the escarpment zone of the continent, due to orographic uplift and the associated wind erosion (Genthon et al., 2009). For example, in the escarpment area of DML, low~~- and-~~ to medium-sized precipitation ~~amounts~~events can be entirely removed by the wind, while high precipitation events lead to net positive SMB (Gorodetskaya et al., 2015). An increase in SMB coupled with an ~~enhanced~~increased wind speed could result in increased SMB where ~~the~~ wind speed is low and decreased SMB ~~in the windier areas (~~where wind speed is high, ~90 % of the Antarctic surface~~,~~ (Frezzotti et al., 2004). Accordingly, Frezzotti et al. (2013) suggested that SMB has increased at low altitude sites and on the highest ridges due to more frequent anticyclonic blocking events, but has decreased at intermediate altitudes due to stronger wind ablation in the escarpment areas. In DML, however, Altnau et al. (2015) reported a SMB increase on the plateau (coupled to an increase in $\delta^{18}O$) and a decrease on coastal sites, which they associated with a change in circulation patterns. Around Dome A, Ding et al. (2011) also reported an increase in SMB in the inland area and a recent decrease towards the coast. Their explanation is that air masses may transfer moisture inland more easily due to climate warming.

Atmospheric circulation exhibits a primary role in determining temporal and spatial SMB variability. Sea-ice and ocean surface conditions play a secondary role, and could contribute to a higher SMB in a warmer climate. A more recent study using a fully coupled climate model (Lenaerts et al., 2016) suggests that DML is the region most susceptible to an increase in snowfall in a present and future warmer climate. The snowfall increase in the coastal regions is particularly attributed to loss of sea ice cover in the Southern Atlantic Ocean, which in turn enhances atmospheric moisture uptake by evaporation. This is further illustrated in Fig. 8, which suggests that extremely high SMB years are associated with low sea ice cover. The longer exposure of open water leads to higher near-surface temperatures and enhances evaporation and moisture availability for ice sheet precipitation (Lenaerts et al., 2016).

5 Conclusions

A 120 m-long ice core was drilled on the ~~divide~~summit of the DIR, and dated ~~back~~ to 1759 ± 16 ~~A.D.~~AD using $\delta^{18}O$, δD, major ion and ECM data. Due to the coastal location of the ice core, the identification of volcanic horizons in the ECM record is hampered by high background acidity. Therefore, we ~~rely on a range of estimates between an~~counted annual layers to develop oldest and ~~a~~ youngest ~~depth-age scale~~age-depth estimates. We combine annual layer thickness with density and thinning functions to calculate ~~the average~~ SMB ~~and temporal trends at this site and their uncertainties.~~time series from the core. The ~~average~~mean SMB ~~between~~for the period 1816–2011 is 0.47 ± 0.02 m w.e. a^{-1} ~~after corrections for densification and dynamic layer thinning. A 32 ± 4 % increase in~~, which increases for more recent time periods such that mean SMB ~~is reconstructed during the 20th and 21st centuries, confirming the relative~~ for the past 20 years (1991 – 2011) rises by 32 ± 3 % to 0.64 ± 0.01 m w.e. a^{-1}. This supports the trend calculated by the CESM for ~~this~~the area. Wind redistribution ~~may well have a substantial impact on interannual variability~~is significant near the ice core location, but this effect appears to have been temporally uniform, giving confidence that the SMB changes we report represent temporal change rather than the effects of local migration in the spatial pattern of SMB~~ at the DIR, but it is unlikely that it has an influence on the temporal trend~~.

SMB trends ~~in SMB~~ observed in other records ~~all over~~across Antarctica are spatially highly variable. In coastal East Antarctica, our study is the only to show an increase in SMB during the ~~20th and 21st centuries.~~past ~100 years. Many studies point to a difference in the behaviour of coastal and inland sites, due to a combination of thermodynamics and dynamic processes. A combination of spatial variability in snowfall and snow redistribution by the wind likely explain ~~the~~much of this observed spatial ~~variations and the poor correlation between our record and the~~variability. Neither currently-available climate ~~reanalyses (ERA-Interim and RACMO2). Our analysis~~models nor reanalysis data are able to resolve ice-rise topography, so detailed predictions from these methods are difficult to match to our ice-core derived SMB time-series. Nevertheless, their temporal trends broadly match those of our reconstructed SMB, and the comparison suggests that SMB variability is governed to a large extent by atmospheric circulation and to a ~~great~~lesser extent ~~determines SMB variability, with a potential secondary role of changes~~by variations in sea ice cover. More studies are needed at other coastal sites in East Antarctica to determine how representative this result ~~is.~~ and our interpretations are.

Long time-series of annual SMB are scarce in coastal East Antarctica. The ~~divide~~summit of Derwael Ice Rise ~~is~~represents a suitable ~~drilling~~ site for deep drilling. It has a relatively high SMB, clear annual layering and appropriate ice conditions (few, thin ice layers) for paleoclimate reconstruction. According to the full Stokes model (Drews et al., 2015), drilling to 350 m could reveal at least 2000 years of a reliable climate record ~~with~~at high resolution, which would address one of the priority targets ("IPICS-2k array", Steig et al., 2005) of the International Partnership in Ice Core Science (IPICS).

Data Availability

~~Age~~Annual layer thicknesses and age–depth data~~ and uncorrected SMB~~ are available online (doi:10.1594/PANGAEA.857574).

Acknowledgements

This paper forms a contribution to the Belgian Research Programme on the Antarctic (Belgian Federal Science Policy Office), Project SD/SA/06A Constraining ice mass changes in Antarctica (IceCon). The authors wish to thank the International Polar Foundation for logistic support in the field. MP is partly funded by a grant from Fonds David et Alice Van Buuren. JTML is funded by Utrecht University through its strategic theme Sustainability, sub-theme Water, Climate and Ecosystems, and the programme of the Netherlands Earth System Science Centre (NESSC), financially supported by the Ministry of Education, Culture and Science (OCW). Ph. C. thanks the Hercules Foundation (www.herculesstichting.be/) for financing the upgrade of the stable isotope laboratory. R. D. was supported by the Deutsche Forschungsgemeinschaft (DFG) in the framework of the priority programme "Antarctic Research with comparative investigations in Arctic ice areas" by the grant MA 3347/10-1. The research leading to these results has received funding from the European Research Council under the European Community's Seventh Framework Programme (FP7/2007-2013) / ERC grant agreement 610055 as part of the Ice2Ice project. Ice coring equipment benefitted from an Aberystwyth University Capital Infrastructure grant and the optical televiewer data from NERC grant NE/J013544/1. The authors also thank Irina Gorodetskaya for her helpful comments and the Norwegian Polar Institute for developing Quantarctica and making this GIS package for Antarctica freely available. The initial version of the manuscript has benefited from the very constructive comments and corrections of two anonymous referees and the Eeditor.

References

Altnau, S., Schlosser, E., Isaksson, E., and Divine, D.: Climatic signals from 76 shallow firn cores in Dronning Maud Land, East Antarctica, The Cryosphere, 9(3), 925-944, doi: 10.5194/tc-9-925-2015, 2015.

Anschütz, H., Müller K., Isaksson, E., McConnell, J. R., Fischer, H., Miller, H., Albert, M., and Winther, J.-G.: Revisiting sites of the South Pole Queen Maud Land Traverses in East Antarctica: accumulation data from shallow firn cores, J. Geophys. Res., 114, D24106, doi: 10.1029/2009JD012204, 2009.

Anschütz, H., Sinisalo, A., Isaksson, E., McConnell, J. R., Hamran, S.-E., Bisiaux, M. M., Pasteris, D., Neumann, T. A., and Winther, J.-G.: Variation of accumulation rates over the last eight centuries on the East Antarctic Plateau derived from volcanic signals in ice cores, J. Geophys. Res., 116, D20103, doi: 10.1029/2011JD015753, 2011.

Arthern, R. J., Vaughan, D. G., Rankin, A. M., Mulvaney, R., and Thomas, E. R.: In situ measurements of Antarctic snow compaction compared with predictions of models, J. Geophys. Res., 115, F03011, doi: 10.1029/2009JF001306, 2010.

Aristarain, A. J., Delmas, R. J., and Stievenard, M.: Ice-core study of the link between sea-salt aerosol, sea-ice cover and climate in the Antarctic Peninsula area, Clim. Change, 67, 63–86, doi: 10.1007/s10584-004-0708-6, 2004.

Boening, C., Lebsock, M., Landerer, F., and Stephens, G.: Snowfall driven mass change on the East Antarctic ice sheet, Geophys. Res. Lett., 39, L21501, doi: 10.1029/2012GL053316, 2012.

Bromwich, D. H., Nicolas, J. P., and Monaghan, A. J.: An assessment of precipitation changes over Antarctica and the Southern Ocean since 1989 in contemporary global reanalyses, J. Clim., 24, 4189–4209, doi: 10.1175/2011jcli4074.1, 2011.

Bromwich, D. H., Nicolas, J. P., Monaghan, A. J., Lazzara, M. A., Keller, L. M., Weidner, G. A., and Wilson, A. B.: Corrigendum: Central West Antarctica among the most rapidly warming regions on Earth. Nature Geoscience, 7(1), 76–76, doi: 10.1038/ngeo2016, 2014.

Callens, D., Drews, R., Witrant, E., Philippe, M., and Pattyn, F.: Temporally stable surface mass balance asymmetry across an ice rise derived from radar internal reflection horizons through inverse modeling, J. Glaciol., doi: 10.1017/jog.2016.41, 2016.

Cuffey, K. M., and Paterson, W.: The ~~physics~~Physics of ~~glaciers~~Glaciers, Elsevier, 693 pp., doi: 10.1016/c2009-0-14802-x, 2010.

Dansgaard, W., and Johnsen, S.: A flow model and a time scale for the ice core from Camp Century, Greenland, J. Glaciol., 8, 215–223, 1969.

Davis, C. H., Li, Y., McConnell, J. R., Frey, M. M., and Hanna, E.: Snowfall-driven growth in East Antarctic Ice Sheet mitigates recent sea-level rise, Science, 308, 1898–1901, doi: 10.1126/science.1110662, 2005.

Ding, M., Xiao, C., Li, Y., Ren, J., Hou, S., Jin, B., and Sun, B.: Spatial variability of surface mass balance along a traverse route from Zhongshan station to Dome A, Antarctica, J. Glaciol., 57, 658–666, doi: 10.3189/002214311797409820, 2011.

Drews, R., Steinhage, D., Martín, C., and Eisen, O.: Characterization of glaciological conditions at Halvfarryggen ice dome, Dronning Maud Land, Antarctica, J. Glaciol., 59 (213), 9–20, doi: 10.3189/2013JoG12J134, 2013.

Drews, R., Matsuoka, K., Martín, C., Callens, D., Bergeot, N., and Pattyn, F.: Evolution of Derwael Ice Rise in Dronning Maud Land, Antarctica, over the last millennia, J. Geophys. Res., Earth Surf., 120, 564–579. doi: 10.1002/2014JF003246, 2015.

Ekaykin, A. A., Lipenkov, V. Y., Kuzmina, I., Petit, J. R., Masson-Delmotte, V., and Johnsen, S. J.: The changes in isotope composition and accumulation of snow at Vostok station, East Antarctica, over the past 200 years, Ann. Glaciol., 39, 569–575, doi: 10.3189/172756404781814348, 2004.

Fernandoy, F., Meyer, H., Oerter, H., Wilhelms, F., Graf, W., and Schwander, J.: Temporal and spatial variation of stable-isotope ratios and accumulation rates in the hinterland of Neumayer station, East Antarctica, J. Glaciol., 56, 673–687, doi: 10.3189/002214310793146296, 2010.

Frezzotti, M., Pourchet, M., Flora, O., Gandolfi, S., Gay, M., Urbini, S., Vincent, C., Becagli, S., Gragnani, R., Proposito, M., Severi, M., Traversi, R., Udisti, R., and Fily, M.: New estimations of precipitation and surface sublimation in East Antarctica from snow accumulation measurements, Clim. Dyn., 23, 803–813, doi: 10.1007/s00382-00004-00462-0038500803-00813, 2004.

Frezzotti, M., Pourchet, M., Flora, O., Gandolfi, S., Gay, M., Urbini, S., Vincent, C., Becagli, S., Gragnani, R., Proposito, M., Severi, M., Traversi, R., Udisti, R., and Fily, M.: Spatial and temporal variability of snow accumulation in East Antarctica from traverse data, J. Glaciol., 51, 113–124, doi: 10.3189/172756505781829502, 2005.

Frezzotti, M., Urbini, S., Proposito, M., Scarchilli, C., and Gandolfi, S.: Spatial and temporal variability of surface mass balance near Talos Dome, East Antarctica, J. Geophys. Res., 112, F02032, doi: 10.1029/2006JF000638, 2007.

Frezzotti, M., Scarchilli, C., Becagli, S., Proposito, M., and Urbini, S.: A synthesis of the Antarctic surface mass balance during the last 800 yr, The Cryosphere, 7, 303–319, doi: 10.5194/tc-7-303-2013, 2013.

Frieler, K., Clark, P. U., He, F., Buizert, C., Reese, R., Ligtenberg, S. R., van den Broeke, M.R., Winkelmann, R., and Levermann, A.: Consistent evidence of increasing Antarctic accumulation with warming, Nat. Clim. Change, 5, 348–352, doi: 10.1038/nclimate2574, 2015.

Fudge, T. J., Markle, B. R. Cuffey, K. M. Buizert, C. Taylor, K. C. Steig, E. J. Waddington, E. D. Conway, H., and Koutnik, M.: Variable relationship between accumulation and temperature in West Antarctica for the past 31,000 years, Geophys. Res. Lett., 43, 3795–3803, doi: 10.1002/2016GL068356, 2016.

Fujita, S., Holmlund, P., Andersson, I., Brown, I., Enomoto, H., Fujii, Y., Fujita, K., Fukui, K., Furukawa, T., Hansson, M., Hara, K., Hoshina, Y., Igarashi, M., Iizuka, Y., Imura, S., Ingvander, S., Karlin, T., Motoyama, H., Nakazawa, F., Oerter, H., Sjöberg, L. E., Sugiyama, S., Surdyk, S., Str¨om, J., Uemura, R., and Wilhelms, F.: Spatial and temporal variability of snow accumulation rate on the East Antarctic ice divide between Dome Fuji and EPICA DML, The Cryosphere, 5, 1057–1081, doi: 10.5194/tc-5-1057-2011, 2011.

Genthon, C., Krinner, G., and Castebrunet, H.: Antarctic precipitation and climate-change predictions: horizontal resolution and margin vs plateau issues, Ann. Glaciol., 50(50), 55-60, doi: 10.3189/172756409787769681, 2009.

Gorodetskaya, I. V., Van Lipzig, N. P. M., Van den Broeke, M. R., Mangold, A., Boot, W., and Reijmer, C. H.: Meteorological regimes and accumulation patterns at Utsteinen, Dronning Maud Land, East Antarctica: Analysis of two contrasting years, J. Geophys. Res.-Atmos., 118, 1700–1715, doi: 10.1002/jgrd.50177, 2013.

Gorodetskaya, I. V., Tsukernik, M., Claes, K., Ralph, M. F., Neff, W. D., and Van Lipzig, N. P. M.: The role of atmospheric rivers in anomalous snow accumulation in East Antarctica, Geophys. Res. Lett., 41, 6199–6206, doi: 10.1002/2014GL060881, 2014.

Gorodetskaya, I. V., Kneifel, S., Maahn, M., Van Tricht, K., Thiery, W., Schween, J. H., Mangold, A., Crewell, S., and Van Lipzig, N. P. M.: Cloud and precipitation properties from ground-based remote-sensing instruments in East Antarctica, The Cryosphere, 9, 285–304, doi:10.5194/tc-9-285-2015, 2015.

Hammer, C.U.: Acidity of polar ice cores in relation to absolute dating, past volcanism, and radio-echoes, J. Glaciol., 25(93), 359–372, doi: 10.3198/1980JoG25-93-359-372, 1980.

Hammer, C. U., Clausen, H. B., and Langway Jr, C. C.: Electrical conductivity method (ECM) stratigraphic dating of the Byrd Station ice core, Antarctica, Ann. Glaciol., 20, 115–120, doi: 10.3189/172756409787769681, 1994.

Hofstede, C. M, van de Wal, R. S. W., Kaspers, K. A., van den Broeke, M. R., Karl¨of, L., Winther, J. G., Isaksson, E., Lappegard, G., Mulvaney, R., Oerther, H., and Wilhelms, F.: Firn accumulation records for the past 1000 years on the basis of dielectric profiling of six firn cores from Dronning Maud Land, Antarctica, J. Glaciol., 50, 279–291, doi: 10.3189/172756504781830169, 2004.

Hubbard, B., Tison, J.-L., Philippe, M., Heene, B., Pattyn, F., Malone, T., and Freitag, J. J.: Ice shelf density reconstructed from optical televiewer borehole logging, Geophys. Res. Lett., 40(22), 5882–5887, doi: 10.1002/2013gl058023, 2013.

Igarashi, M., Nakai, Y., Motizuki, Y., Takahashi, K., Motoyama, H., and Makishima, K.: Dating of the Dome Fuji shallow ice core based on a record of volcanic eruptions from AD 1260 to AD 2001, Polar Sci., 5, 411–420, doi: 10.1016/j.polar.2011.08.001, 2011.

Isaksson, E., and Melvold, K.: Trends and patterns in the recent accumulation and oxygen isotope in coastal Dronning Maud Land, Antarctica: interpretations from shallow ice cores, Ann. Glaciol., 35, 175–180, doi: 10.3189/172756402781817356, 2002.

Isaksson, E., Karlén, W., Gundestrup, N., Mayewski, P., Whitlow, S., and Twickler, M.: A century of accumulation and temperature changes in Dronning Maud Land, Antarctica, J. Geophys. Res., 101, 7085–7094, doi: 10.1029/95jd03232, 1996.

Isaksson, E., van den Broeke, M. R., Winther, J.-G., Karlöf, L., Pinglot, J. F., and Gundestrup, N.: Accumulation and proxytemperature variability in Dronning Maud Land, Antarctica, determined from shallow firn cores, Ann. Glaciol., 29, 17–22, doi: 10.3189/172756499781821445, 1999.

ISMASS Committee: Recommendations for the collection and synthesis of Antarctic Ice Sheet mass balance data, Global Planet. Change, 42, 1–15, doi:10.1016/j.gloplacha.2003.11.008, 2004.

Jiang, S., Cole-Dai, J., Li, Y., Ferris, D.G., Ma, H., An, C., Shi, G., and Sun, B.: A detailed 2840 year record of explosive volcanism in a shallow ice core from Dome A, East Antarctica, J. Glaciol., 58, 65–75, doi: 10.3189/2012JoG11J138, 2012.

Kaczmarska, M., Isaksson, E., Karlöf, K., Winther, J-G, Kohler, J., Godtliebsen, F., Ringstad Olsen, L., Hofstede, C. M., van den Broeke, M. R., Van DeWal, R. S.W., and Gundestrup, N.: Accumulation variability derived from an ice core from coastal Dronning Maud Land, Antarctica, Ann. Glaciol., 39, 339–345, doi: 10.3189/172756404781814186, 2004.

Karlöf, L., Winther, J. G., Isaksson, E., Kohler, J., Pinglot, J. F., Wilhelms, F., Hansson, M., Holmlund, P., Nyman, M., Pettersson, R., Stenberg, M., Thomassen, M. P. A., van der Veen, C., and van de Wal, R. S. W.: A 1500 year record of accumulation at Amundsenisen western Dronning Maud Land, Antarctica, derived from electrical and radioactive measurements on a 120 m ice core, J. Geophys. Res., 105(D10), 12471–12483, doi: 10.1029/1999JD901119, 2000.

Karlof, L., Isakson, E., Winther, J. G., Gundestrup, N., Meijer, H. A. J., Mulvaney, R., Pourcher, M., Hofstede, C., Lappegard, G., Petterson, R., van den Broecke, M. R., and van de Wal, R. S. W.: Accumulation variability over a small area in east Dronning Maud Land, Antarctica, as determined from shallow firn cores and snow pits: some implications for ice, J. Glaciol., 51, 343–352, doi: 10.3189/172756505781829232, 2005.

Kaspari, S., Mayewski, P. A., Dixon, D. A., Spikes, V. B., Sneed, S. B., Handley, M. J., and Hamilton, G. S.: Climate variability in west Antarctica derived from annual accumulation-rate records from ITASE firn/ice cores, Ann. Glaciol., 39, 585–594, doi: 10.3189/172756404781814447, 2004.

King, M. A., Bingham, R. J., Moore, P., Whitehouse, P. L., Bentley, M. J., and Milne, G. A.: Lower satellite-gravimetry estimates of Antarctic sea-level contribution, Nature, 491, 586–589, doi: 10.1038/nature11621, 2012.

Kingslake, J., R. C. A. Hindmarsh, G. Aðalgeirsdóttir, H. Conway, H. F. J. Corr, F. Gillet-Chaulet, C. Martín, E. C. King, R. Mulvaney, and H. D. Pritchard: Full-depth englacial vertical ice sheet velocities measured using phase-sensitive radar, J. Geophys. Res.: Earth Surface, 119(12), 2604-2618, doi: 10.1002/2014jf003275, 2014.

Kjaer, H., Vallelonga, P., Svensson, A., Elleskov, L., Kristensen, M., Tibuleac, C., Winstrup, M., and Kipfstuhl, S.: An optical dye method for continuous determination of acidity in ice cores, Environ. Sci. Technol., ~~es-2016-00026e, *in review*.~~doi: 10.1021/acs.est.6b00026, 2016

Krinner, G., Magand, O., Simmonds, I., Genthon, C., and Dufresne, J. L.: Simulated Antarctic precipitation and surface mass balance at the end of the 20th and 21th centuries, Clim. Dynam. 28, 215–230, doi: 10.1007/s00382-006-0177-x, 2007.

Lenaerts, J. T. M., van den Broeke, M. R., van den Berg, W. J., van Meijgaard, E., and Munneke, P. K.: A new, high resolution surface mass balance map of Antarctica (1979–2010) based on regional climate modeling, Geophys. Res. Lett., 39, L04501, doi: 10.1029/2011GL050713, 2012.

Lenaerts, J. T. M., van Meijgaard, E., van den Broeke, M. R., Ligtenberg, S. R. M., Horwath, M., and Isaksson, E.: Recent snowfall anomalies in Dronning Maud Land, East Antarctica, in a historical and future climate perspective, Geophys. Res. Lett., 40, 1–5, doi-: 10.1002/grl.50559, 2013.

Lenaerts, J.T.M., Brownvan, J., den Broeke, M. R., Matsuoka, K., Drews, R., Callens, D., Philippe, M., Gorodetskaya, I., van Meijgaard, E., Reymer, C., Pattyn, F., and van Lipzig, N. P.: High variability of climate and surface mass balance induced by Antarctic ice rises, J. Glaciol., 60(224): 1101–1110, doi: 10.3189/2014jog14j040, 2014.

Lenaerts, J. T. M., Vizcaino, M., Fyke, J.,van Kampenhout, L., and van den Broeke, M. R.: Present-day and future Antarctic ice sheet climate and surface mass balance in the Community Earth System Model, Clim. Dynam., online first, doi: 10.1007/s00382-015-2907-4, 2016.

Levasseur, M.: Impact of Arctic meltdown on the microbial cycling of sulphur, Nat. Geosci., 6, 691–700, doi: 10.1038/ngeo1910, 2013.

Ludescher, J., Bunde, A., Franzke, C. L., and Schellnhuber, H. J.: Long-term persistence enhances uncertainty about anthropogenic warming of Antarctica, Clim. Dyn., 1–9, doi: 10.1007/s00382-015-2582-5, 2015.

Magand, O., Frezzotti, M., Pourchet, M., Stenni, B., Genoni, L., and Fily, M.: Climate variability along latitudinal and longitudinal transects in east Antarctica, Ann. Glaciol., 39, 351–358, doi: 10.3189/172756404781813961, 2004.

Magand, O., Genthon, C., Fily, M., Krinner, G., Picard, G., Frezzotti, M., and Ekaykin, A. A.: An up-to-date quality-controlled surface mass balance data set for the 90–180E Antarctica sector and 1950–2005 period, J. Geophys. Res., 112, D12106, doi: 10.1029/2006JD007691, 2007.

Marshall, G. J.: Trends in the southern annular mode from observations and reanalyses, J. Climate, 16, 4134–4143, ~~2003.~~doi: 10.1175/1520-0442(2003)016<4134:titsam>2.0.co;2, 2003.

Matsuoka, K., Hindmarsh, R. C., Moholdt, G., Bentley, M. J., Pritchard, H. D., Brown, J., Conway, H., Drews, R., Durand, G., Goldberg, D., Hattermann, T., Kingslake, J., Lenearts, J., Martin, C., Mulvaney, R., Nicholls, K., Pattyn, F., Ross, N., Scambos, T., and Whitehouse, P.: Antarctic ice rises and rumples: their properties and significance for ice-sheet dynamics and evolution. Earth-Sci. Rev., 150, 724–745, doi: 10.1016/j.earscirev.2015.09.004, 2015.

Medley, B., Joughin, I., Das, S. B., Steig, E. J., Conway, H., Gogineni, S., Criscitiello, A. S., McConnell, J. R., Smith, B. E., van den Broeke, M. R., Lenaerts, J. T. M., Bromwich, D. H., and Nicolas, J. P.: Airborne-radar and ice-core observations of annual snow accumulation over Thwaites Glacier, West Antarctica confirm the spatiotemporal variability of global and regional atmospheric models, Geophys. Res. Lett., 40(14), 3649–3654, doi: 10.1002/grl.50706, 2013.

Monaghan, A. J., Bromwich, D. H., Fogt, R. L., Wang, S., Mayewski, P. A., Dixon, D. A., Ekaykin, A., Frezzotti, M., Goodwin, I., Isaksson, E., Kaspari, S. D., Morgan, V. I., Oerter, H., Van Ommen, T. D., van der Veen, C. J., and Wen, J.: Insignificant change in Antarctic snowfall since the International Geophysical Year, Science, 313, 827–831, doi: 10.1126/science.1128243, 2006.

Moore, J. C., Narita, H., and Maeno, N.: A continuous 770-year record of volcanic activity from East Antarctica, J. Geophys. Res., 96, 17353–17359, doi: 10.1029/91jd01283, 1991.

Morgan, V. I., Goodwin, I. D., Etheridge, D. M., and Wookey, C. W.: Evidence from Antarctic ice cores for ~~increased~~recent increases in snow accumulation~~ in Antarctica~~, Nature, 354~~,~~(6348), 58–60, doi: 10.1038/354058a0, 1991.

Mosley-Thompson, E., Paskievitch, J. F., Gow, A. J., and Thompson, L. G.: Late 20th century increase in South Pole snow accumulation, J. Geophys. Res., 104, 3877–3886, doi: 10.1029/1998jd200092, 1999.

Mulvaney, R., Pasteur, E.C. and Peel, D.A.: The ratio of MSA to non sea-salt sulphate in Antarctic peninsula ice cores, Tellus, 44b, 293-303, doi: 10.3402/tellusb.v44i4.15457, 1992.

Mulvaney, R., Oerter, H., Peel, D. A., Graf, W., Arrowsmith, C., Pasteur, E. C., Knight, B., Littot, G. C., and Miners, W. D: 1000-year ice core records from Berkner Island, Antarctic, Ann. Glaciol., 35, 45–51, doi: 10.3189/172756402781817176, 2002.

Nishio, F., Furukawa, T., Hashida, G., Igarashi, M., Kameda, T., Kohno, M., Motoyama, H., Naoki, K., Satow, K., Suzuki, K., Morimasa, T., Toyama, Y., Yamada, T., and Watanabe, O.: Annual-layer determinations and 167 year records of past climate of H72 ice core in east Dronning Maud Land, Antarctica, Ann. Glaciol., 35, 471–479, doi: 10.3189/172756402781817086, 2002.

Oerter, H., Graf, W., Wilhelms, F., Minikin, A., and Miller, H.: Accumulation studies on Amundsenisen, Dronning Maud Land, by means of tritium, DEP and stable isotope measurements: first results from the 1995/96 and 1996/97 field seasons, Ann. Glaciol., 29, 1–9, doi: 10.3189/172756499781820914, 1999.

Oerter, H., Wilhelms, F., Jung-Rothenhausler, F., Goktas, F., Miller, H., Graf, W., and Sommer, S.: Accumulation rates in Dronning Maud Land as revealed by DEP measurements at shallow firn cores, Ann. Glaciol., 30, 27–34, doi: 10.3189/172756400781820705, 2000.

Palerme, C., Genthon, C., Claud, C., Kay, J. E., Wood, N. B. and L'Ecuyer, T.: Evaluation of current and projected Antarctic precipitation in CMIP5 models, Clim.Dyn., online first, doi:10.1007/s00382-016-3071-1, 2016.

Parrenin, F., Dreyfus, G., Durand, G., Fujita, S., Gagliardini, O., Gillet, F., Jouzel, J., Kawamura, K., Lhomme, N., Masson-Delmotte, V., Ritz, C., Schwander, J., Shoji, H., Uemura, R., Watanabe, O., and Yoshida, N.: 1-D-ice flow modelling at EPICA Dome C and Dome Fuji, East Antarctica, Clim. Past, 3, 243–259, doi: 10.5194/cp-3-243-2007, 2007.

Philippe, M., Hubbard, B., Pattyn, F., Fjøsne, K., Drews, R., Bruyninx, C., Bergeot, N. and Tison, J.-L. : Vertical velocities of firn and ice reconstructed from optical televiewer borehole logging at Derwael ice rise, Princess Ragnhild Coast, Antarctica, *in prep.*

Raymond, C.,Weertman, B., Thompson, L., Mosley-Thompson, E., Peel, D., and Mulvaney, R.: Geometry, motion and mass balance of Dyer Plateau, Antarctica, J. Glaciol., 42, 510–518, doi: 10.3198/1996JoG42-142-510-518, 1996.

Ren, J., Li, C., Hou, S., Xiao, C., Qin, D., Li, Y., and Ding, M.: A 2680 year volcanic record from the DT-401 East Antarctic ice core, J. Geophys. Res., 115, D11301, doi: 10.1029/2009JD012892, 2010.

Rignot, E., Velicogna, I., van den Broeke, M. R., Monaghan, A., and Lenaerts, J.: Acceleration of the contribution of the Greenland and Antarctic ice sheets to sea level rise, Geophys. Res. Lett., 38, L05503, doi: 10.1029/2011GL046583, 2011.

Roberts, J., Plummer, C., Vance, T., van Ommen, T., Moy, A., Poynter, S., Treverrow, A., Curran, M., and George, S.: A 2000-year annual record of snow accumulation rates for Law Dome, East Antarctica, Clim. Past, 11, 697–707, doi: 10.5194/cp-11-697-2015, 2015.

Rupper, S., Christensen, W. F., Bickmore, B. R., Burgener, L., Koenig, L. S., Koutnik, M. R., Miège, C., and Forster, R. R.: The effects of dating uncertainties on net accumulation estimates from firn cores. J. Glaciol., 61(225), 163–172, doi: 10.3189/2015jog14j042, 2015.

Ruth, U., Wagenbach, D., Mulvaney, R., Oerter, H., Graf, W., Pulz, H., and Littot, G.: Comprehensive 1000 year climate history from an intermediate depth ice core from the south dome of Berkner Island, Antarctica: methods, dating and first results, Ann. Glaciol., 39, 146–154, doi: 10.3189/172756404781814104, 2004.

Savitzky A., and Golay, M. J. E.: Smoothing and Differentiation of Data by Simplified Least Squares Procedures. Anal. Chem., 36 (8), pp 1627–1639, ~~DOI~~doi: 10.1021/ac60214a047, 1964.

Schlosser, E., and Oerter, H.: Shallow firn cores from Neumayer, Ekströmisen, Antarctica: a comparison of accumulation rates and stable-isotope ratios, Ann. Glaciol., 35, 91–96, doi: 10.3189/172756402781816915, 2002.

Schlosser, E., Manning, K. W., Powers, J. G., Duda, M. G., Birnbaum, G., and Fujita, K.: Characteristics of high-precipitation events in Dronning Maud Land, Antarctica, J. Geophys. Res., 115, D14107, doi: 10.1029/2009JD013410, 2010.

Schlosser, E., Anschütz, H., Divine, D., Martma, T., Sinisalo, A., Altnau, S., and Isaksson, E.: Recent climate tendencies on an East Antarctic ice shelf inferred from a shallow firn core network, J. Geophys. Res., 119, 6549–6562, doi: 10.1002/2013jd020818, 2014.

Shepherd, A., Ivins, E. R., Geruo, A., Barletta, V. R., Bentley, M. J., Bettadpur, S., Briggs, K. H., Bromwich, D. H., Forsberg, R., Galin, N., Horwath, M., Jacobs, S., Joughin, I., King, M. A., Lenaerts, J. T. M., Li, J., Ligtenberg, S. R. M., Luckman, A., Luthcke, S. B., McMillan, M., Meister, R., Milne, G., Mouginot, J., Muir, A., Nicolas, J. P., Paden, J., Payne, A. J., Pritchard, H., Rignot, E., Rott, H., Sørensen, L. S., Scambos, T. A., Scheuchl, B., Schrama, E. J. O., Smith, B., Sundal, A. V., van Angelen, J. H., van de Berg, W. J., van den Broeke, M. R., Vaughan, D. G., Velicogna, I., Wahr, J., Whitehouse, P. L., Wingham, D. J., Yi, D., Young, D., and Zwally, H. J.: A reconciled estimate of ice-sheet mass balance, Science, 338(6111), 1183–1189, doi: 10.1126/science.1228102, 2012.

Sigl, M., McConnell, J. R., Layman, L., Maselli, O., McGwire, K., Pasteris, D., Dahl-Jensen, D., Steffensen, J. P., Vinther, B., Edwards, R., Mulvaney, R, and Kipfstuhl, S.: A new bipolar ice core record of volcanism from WAIS Divide and NEEM and implications for climate forcing of the last 2000 years. Journal of Geophysical Research: Atmospheres, 118(3), 1151-1169, doi: 10.1029/2012jd018603, 2013.

Sommer, S., Appenzeller, C., Röthlisberger, R., Hutterli, M. A., Stauffer, B.,Wagenbach, D., Oerter, H.,Wilhelms, F., Miller, H., and Mulvaney, R.: Glacio-chemical study spanning the past 2 kyr on three ice cores from Dronning Maud Land, Antarctica, 1. Annually resolved accumulation rates, J. Geophys. Res., 105, 29411–29421, doi: 10.1029/2000jd900449, 2000.

Steig, E., Fischer, H., Fisher, D., Frezzotti, M., Mulvaney, R., Taylor, K., Wolff, E.: The IPICS 2k Array: a network of ice core climate and climate forcing records for the last two millennia, http://www.pages-igbp.org/ipics/ IPICS (International Partnership in Ice Core Science), 2005.

Stenni, B., Caprioli, R., Cimmino, L., Cremisini, C., Flora, O., Gragnani, R., Longinelli, A., Maggi, V., and Torcini, S.: 200 years of isotope and chemical records in a firn core from Hercules Neve, northern Victoria Land, Antarctica, Ann. Glaciol., 29, 106–112, doi: 10.3189/172756499781821175, 1999.

Takahashi, H., Yokoyama, T., Igarashi, M., Motoyama, H., and Suzuki, K.: Resolution of environmental variation by detail analysis of YM85 shallow ice core in Antarctica, Bull. Glaciol. Res., 27, 16–23, 2009.

Thomas, E. R., Marshall, G. J., and McConnell, J. R.: A doubling in snow accumulation in the western Antarctic Peninsula since 1850, Geophys. Res. Lett., 35, L01706, doi: 10.1029/2007GL032529, 2008.

Thomas, E. R., Hosking, J. S., Tuckwell, R. R., Warren, R.A., and Ludlow, E.C.: Twentieth century increase in snowfall in coastal West Antarctica, Geophys. Res. Lett., 42, 9387–9393, doi: 10.1002/2015GL065750, 2015.

Traufetter, F., Oerter, H., Fischer, H., Weller, R., and Miller, H.: Spatio-temporal variability in volcanic sulphate deposition over the past 2 kyr in snow pits and firn cores from Amundsenisen, Antarctica., J. Glaciol., 50(168), 137–146, doi: 10.3189/172756504781830222, 2004.

Turner, J., Colwell, S. R., Marshall, G. J., Lachlan-Cope, T. A., Carleton, A. M., Jones, P. D., Lagun, V., Reid, P. A. and Iagovkina, S.: Antarctic climate change during the last 50 years, Int. J. Climatol., 25: 279–294, doi: 10.1002/joc.1130, 2005.

van de Berg, W. J., van den Broeke, M. R., Reijmer, C. H., and van Meijgaard, E.: Reassessment of the Antarctic SMB using calibrated output of a regional atmospheric climate model, J. Geophys. Res., 111, D11104, doi: 10.1029/2005JD006495, 2006.

van den Broeke, M., van de Berg, W. J., and van Meijgaard, E.: Snowfall in coastal West Antarctica much greater than previously assumed, Geophys. Res. Lett., 33, L02505, doi: 10.1029/2005GL025239, 2006.

van Ommen, T. D., and Morgan, V.: Snowfall increase in coastal East Antarctica linked with southwest Western Australian drought, Nat. Geosci., 3, 267–272, doi: 10.1038/ngeo761, 2010.

Vaughan, D.G., Comiso, J.C., Allison, I., Carrasco, J., Kaser, G., Kwok, R., Mote, P., Murray, T., Paul, F., Ren, J., Rignot, E., Solomina, O., Steffen, K., and Zhang, T.: Observations: Cryosphere. In: Climate Change 2013: The Physical Science Basis. Contribution of Working Group I to the Fifth Assessment Report of the Intergovernmental Panel on Climate Change [Stocker, T.F., D. Qin, G.-K. Plattner, M. Tignor, S.K. Allen, J. Boschung, A. Nauels, Y. Xia, V. Bex and P.M. Midgley (eds.)]. Cambridge University Press, Cambridge, United Kingdom and New York, NY, USA, 2013.

Wang, Y., Ding, M., van Wessem, J., Schlosser, E., Altnau, S., van den Broeke, M., Lenaerts, J., Thomas, E., Isaksson, E., Wang, J., and Sun, W.: A comparison of Antarctic Ice Sheet surface mass balance from atmospheric climate models and in situ observations, J. Climate, doi: 10.1175/JCLI-D-15-0642.1, early online release, 2016.

Wolff, E. W., Jones, A. E., Bauguitte, S. B., and Salmon, R. A.: The interpretation of spikes and trends in concentration of nitrate in polar ice cores, based on evidence from snow and atmospheric measurements, Atmos. Chem. Phys., 8(18), 5627–5634, doi: 10.5194/acp-8-5627-2008, 2008.

Xiao, C., Mayewski, P. A., Qin, D., Li, Z., Zhang, M., and Yan, Y.: Sea level pressure variability over the southern Indian Ocean inferred from a glaciochemical record in Princess Elizabeth Land, east Antarctica, J. Geophys. Res., 109, D16101, doi: 10.1029/2003JD004065, 2004.

Zhang, M., Li, Z., Ren, J., Xiao, C., Qin, D., Kang, J., and Li, J.: 250 years of accumulation, oxygen isotope and chemical records in a firn core from Princess Elizabeth Land, East Antarctica, J. Geogr. Sci., 16, 23–33, doi: 10.1007/s11442-006-0103-5, 2006.

Tables

Table 1. Mean SMB at IC12 for different time periods. These values may be compared with those of several published studies, summarized in Table A1.

Period (years ~~A.D.)~~AD)	**SMB (m w.e. a^{-1}) (oldest estimate)**	**SMB (m w.e. a^{-1}) (youngest estimate)**	**Mean SMB (m w.e. a^{-1})**
1816–2011	0.476	0.513	0.495
1816–1900	0.401	0.441	0.421
1900–2011	0.532	0.568	0.550
1816–1961	0.432	0.476	0.454
1962–2011	0.604	0.623	0.614
1816–1991	0.459	0.498	0.479
1992–2011	0.626	0.651	0.638

Table 2. SMB of the last 10 years from IC12 ice core (oldest and youngest estimates, see text for details)

Year (~~A.D.)~~AD)	**SMB (m w.e. a^{-1}) (oldest estimate)**	**SMB (m w.e. a^{-1}) (youngest estimate)**
2011	0.980	0.980
2010	0.641	0.641
2009	0.824	0.824
2008	0.651	0.651
2007	0.287	0.699
2006	0.419	0.661
2005	0.661	0.681
2004	0.681	0.666
2003	0.666	0.621
2002	0.621	0.891

Figures

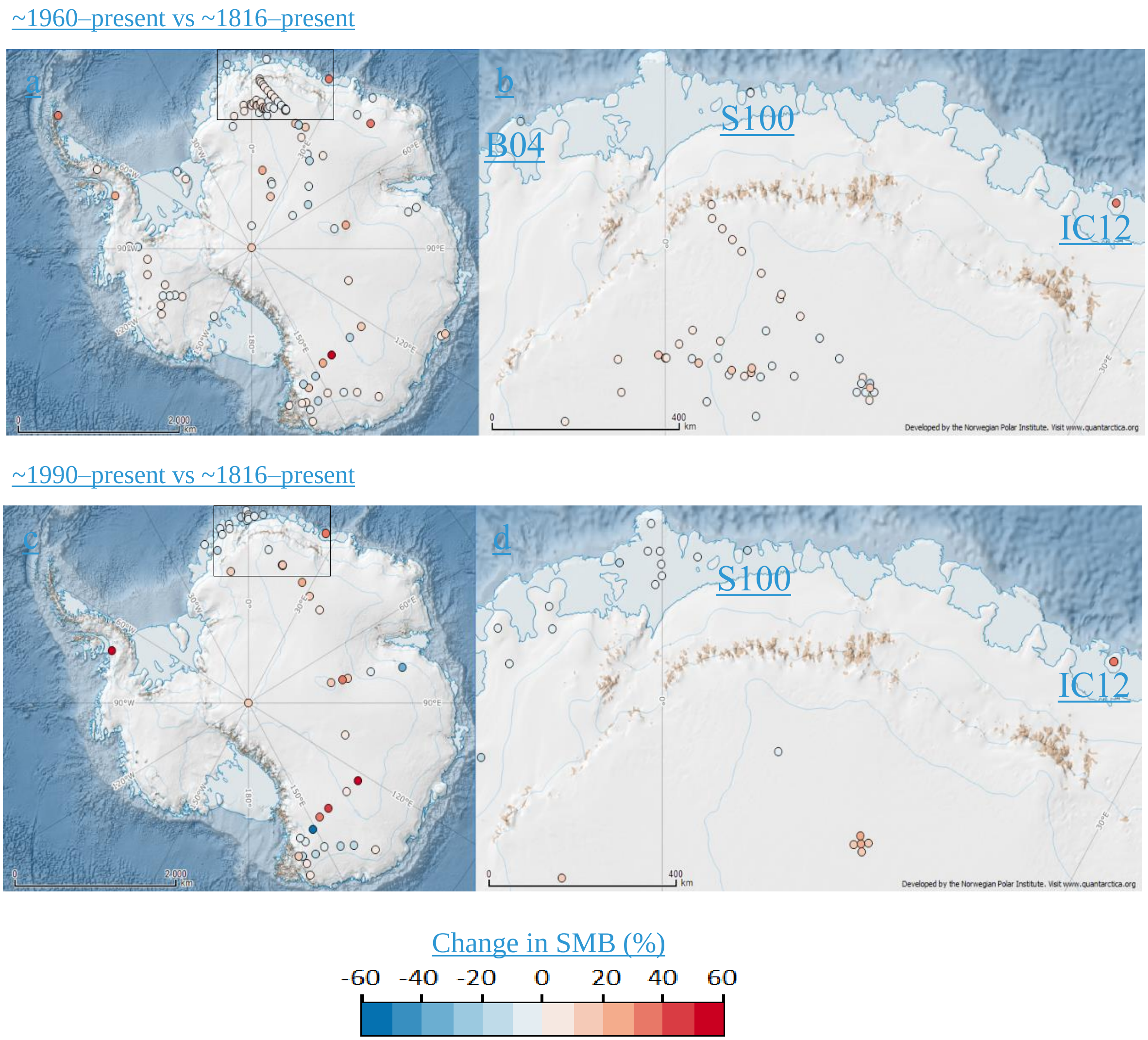

Fig. 1: Location of IC12 and other ice cores referred to herein. (a-b) Difference in mean annual SMB between the period ~1960–present and the period ~1816–present (see Table A1 for exact periods); (c-d) Same as (a-b) for the period ~1990–present compared to ~1816–present. Panels (b) and (d) are expansions of the framed areas in panels (a) and (c).

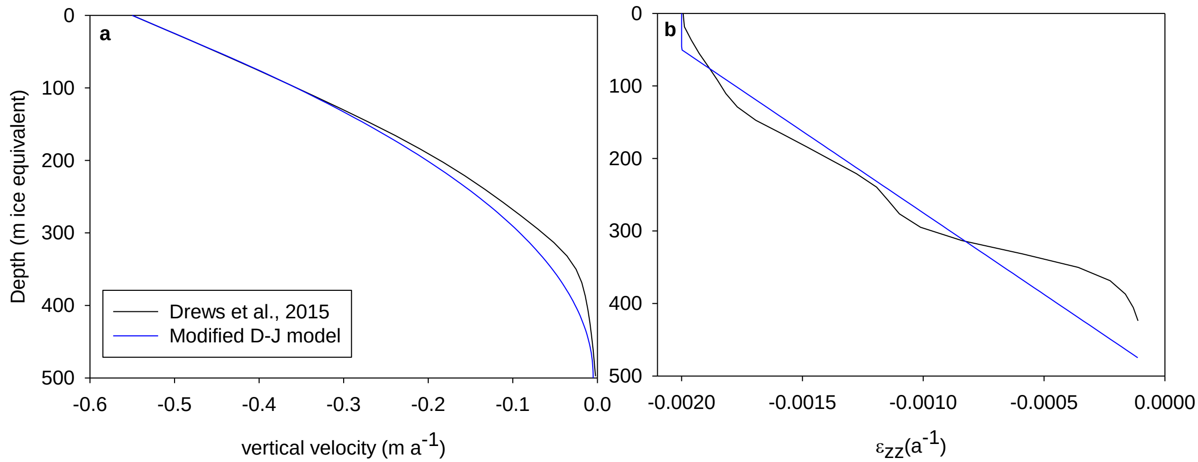

Fig. 2. (a) Vertical velocity profiles, according to the modified Dansgaard–Johnsen model (blue) and the full stokes model (black, Drews et al., 2015). (b) Same as (a) for the vertical strain rate profiles.

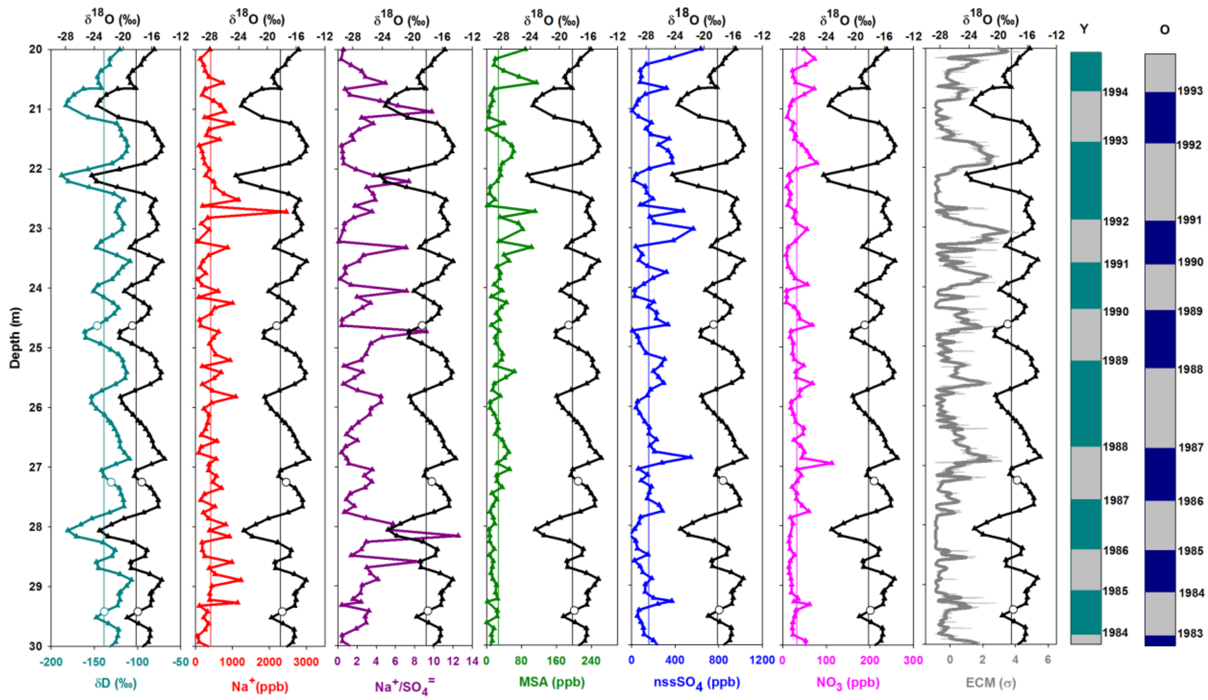

Fig. 3. A 10 m-‐-long illustrative example of how variations in stable isotopes ($\delta^{18}O$, δD), chemical species (or their ratios) and smoothed ECM (running mean, 0.1 m) are used to identify annual layers. Coloured bars on the right indicate the annual layer boundaries (middle depth of each period corresponding to above average $\delta^{18}O$ values) for the youngest (Y) and oldest (O) estimates, with 1 year difference at 20 m depth. See ~~Fig.~~Figs S1 and S2 for the whole profile. White dots in the $\delta^{18}O$ and δD profiles indicate thin ice layers identified visually in the core. $\delta^{18}O$ profiles are shown multiple times to better illustrate correlations between $\delta^{18}O$ and other profiles.

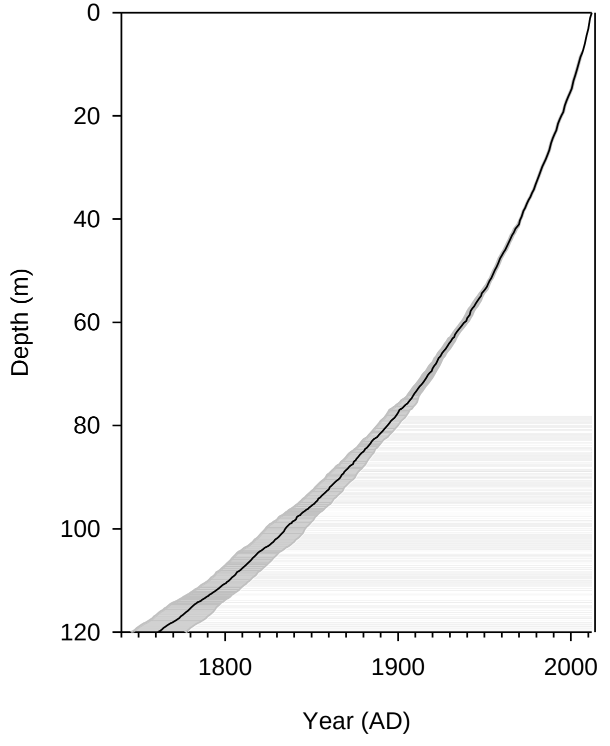

Fig. 4. Age–depth relationship for IC12 reconstructed from the relative dating process. Grey shading shows the uncertainty range between the oldest and the youngest estimates. ~~At the bottom, the~~ The uncertainty ~~is~~range reaches a maximum of ± 16 years at the base of the core.

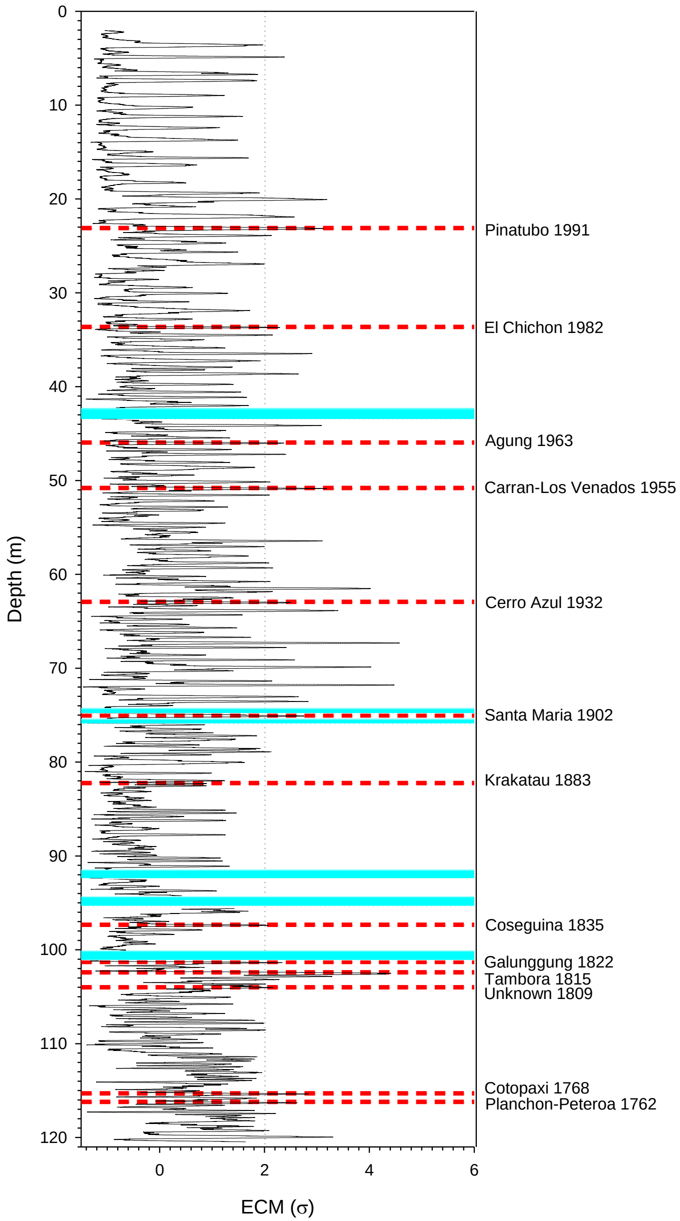

Fig. 5. Continuous record of ECM (except for ~~6~~six measurement gaps shown as ~~grey~~cyan bands). Normalized conductivity (black line) is expressed as multiple of standard deviation (σ). The 2σ threshold is shown as a dotted vertical line, and identified volcanic peaks as dashed ~~grey~~red horizontal lines.

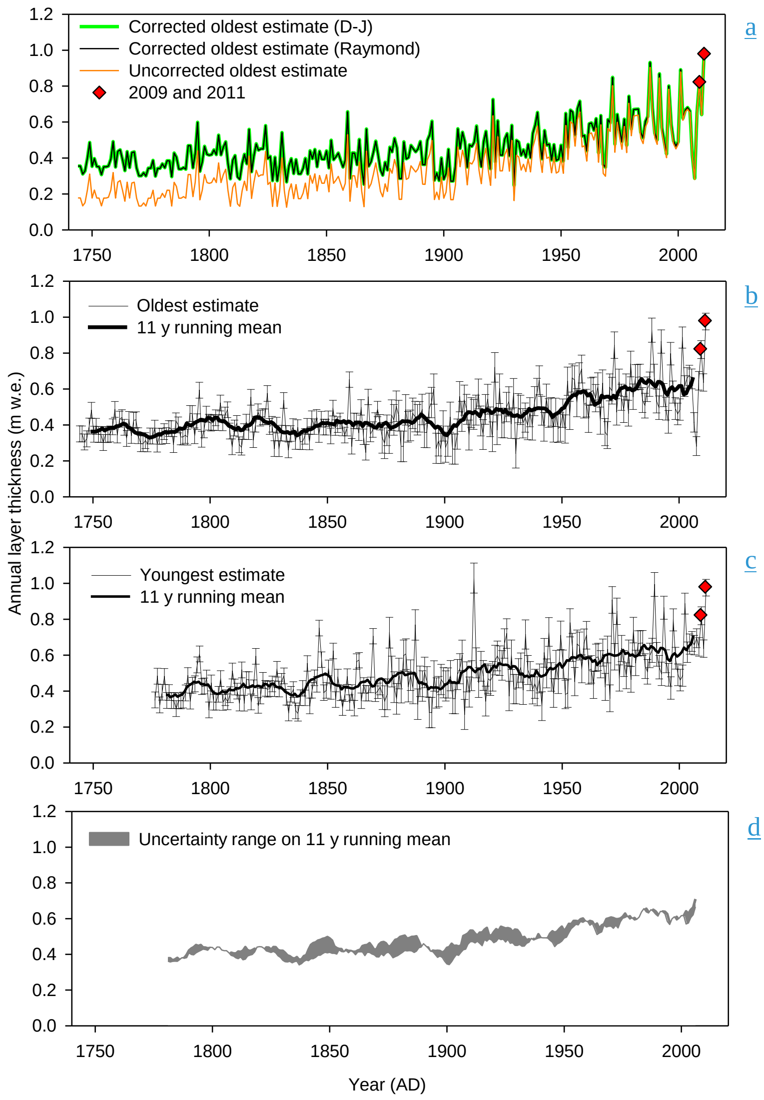

Fig. 6. Annual layer thicknesses at IC12 in m w.e.: (a) for the oldest estimate: uncorrected annual layer thickness (orange line), corrected annual layer thickness using full stokes Drews et al. (2015) model (black line) and corrected annual layer thickness with the modified Dansgaard–Johnsen model (green line, undistinguishable from the black line at this scale); (b) corrected annual layer thickness using Drews et al. (2015) model with error bars, showing 5-10 cm depth uncertainty (thin black line) and 11 year running mean (thick black line) for the oldest estimate; (c) Same as (b) for the youngest estimate (c); (d) Range of uncertainty between youngest and oldest estimates (11 year running mean). Red diamonds highlight years 2009 and 2011, discussed in the text.

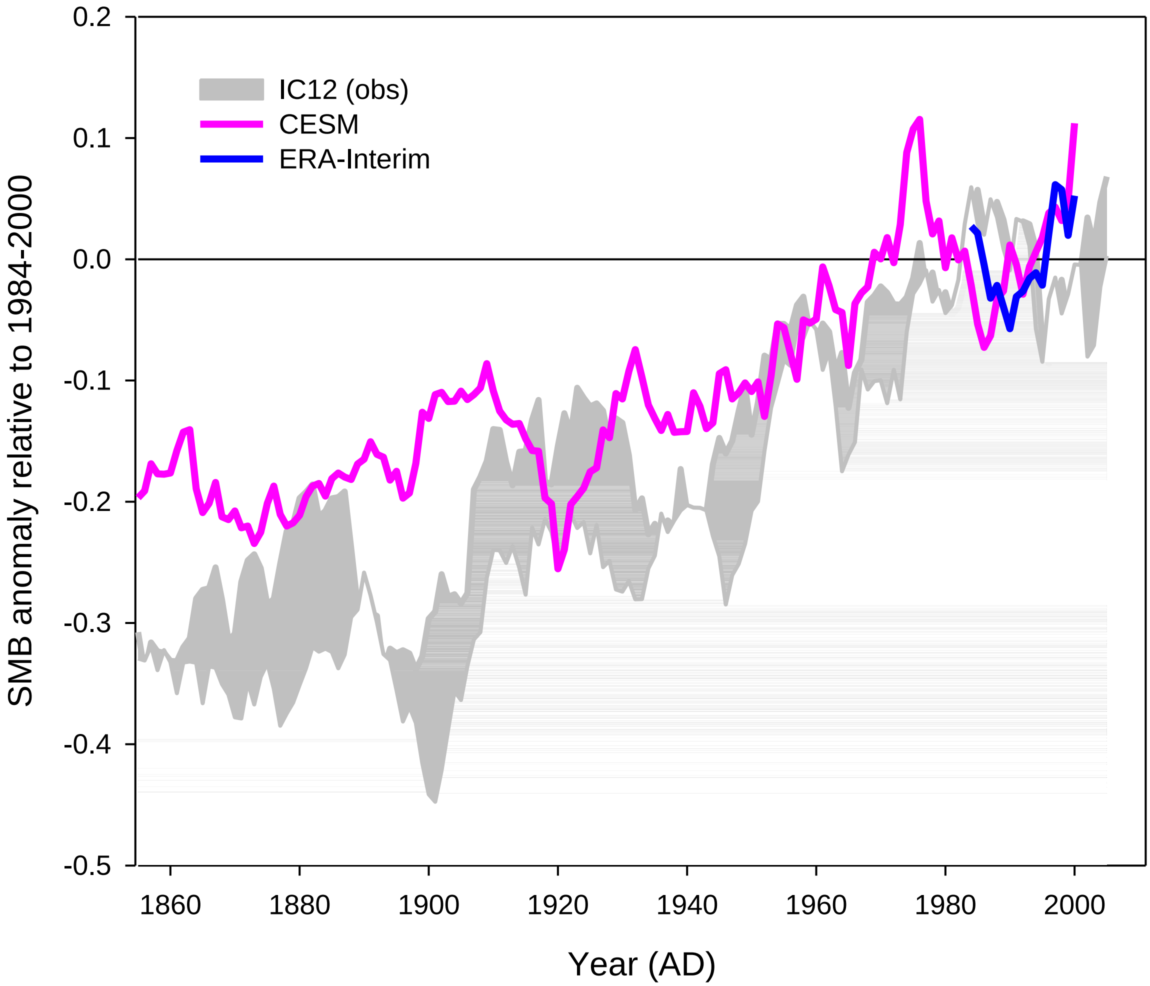

Fig. 7. Comparison between trends in IC12 record (range between youngest (upper boundary) and oldest estimate (lower boundary), shown as grey band), CESM output (pink ~~line~~curve) and ERA-Interim reanalysis (blue ~~line~~curve) represented as relative anomaly compared to 1979–1989 (black line), for the overlapping period 1850–2011.

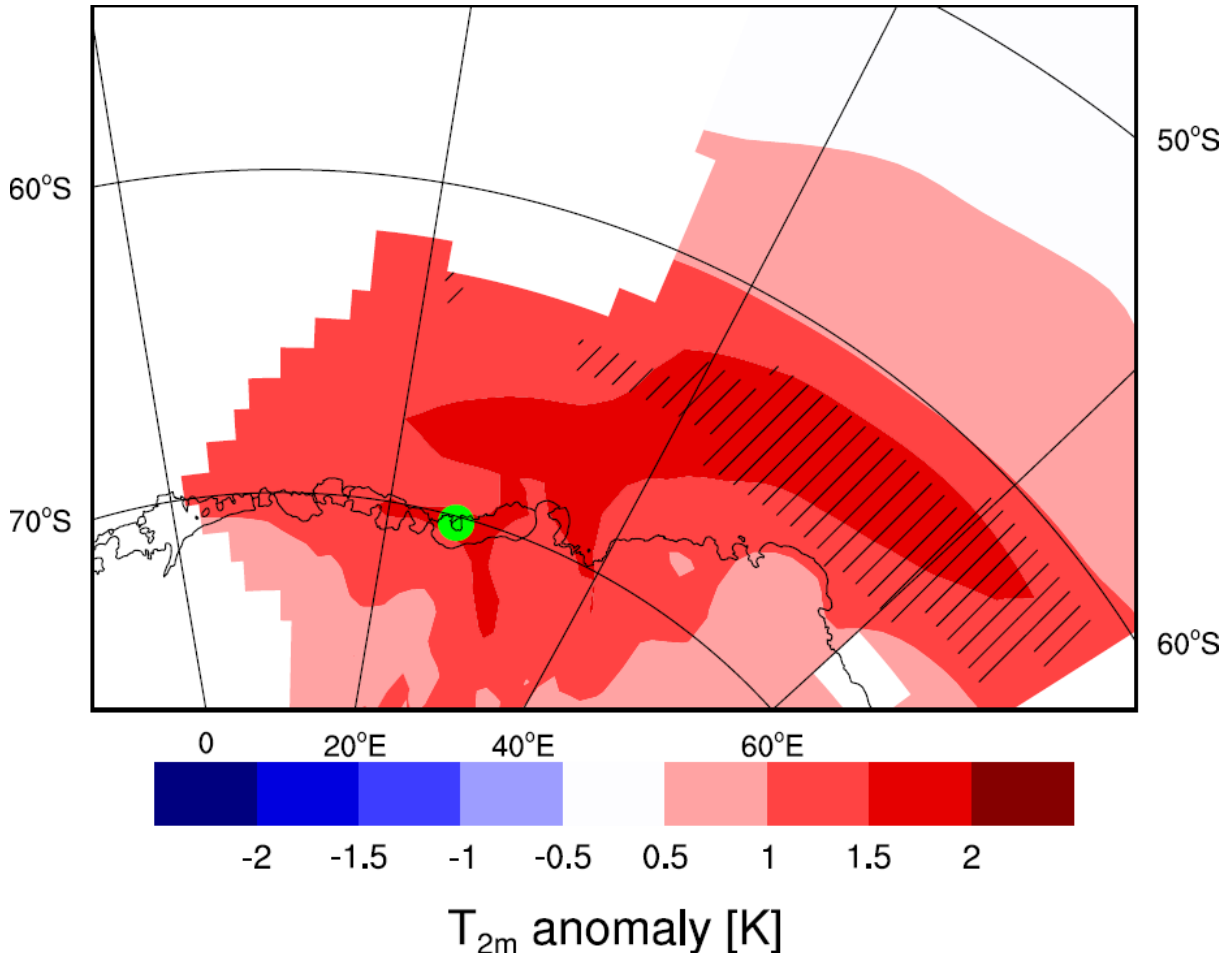

Fig. 8. Large-scale atmospheric, ocean and sea-ice anomalies in high-SMB (10 % highest) years in the CESM historical time series (1850–2005). The colours show the annual mean near-surface temperature anomaly (in °C), and the hatched areas show the anomaly in sea-ice coverage (>20 days less sea ice cover than the mean). The green dot shows the location of the ice core.

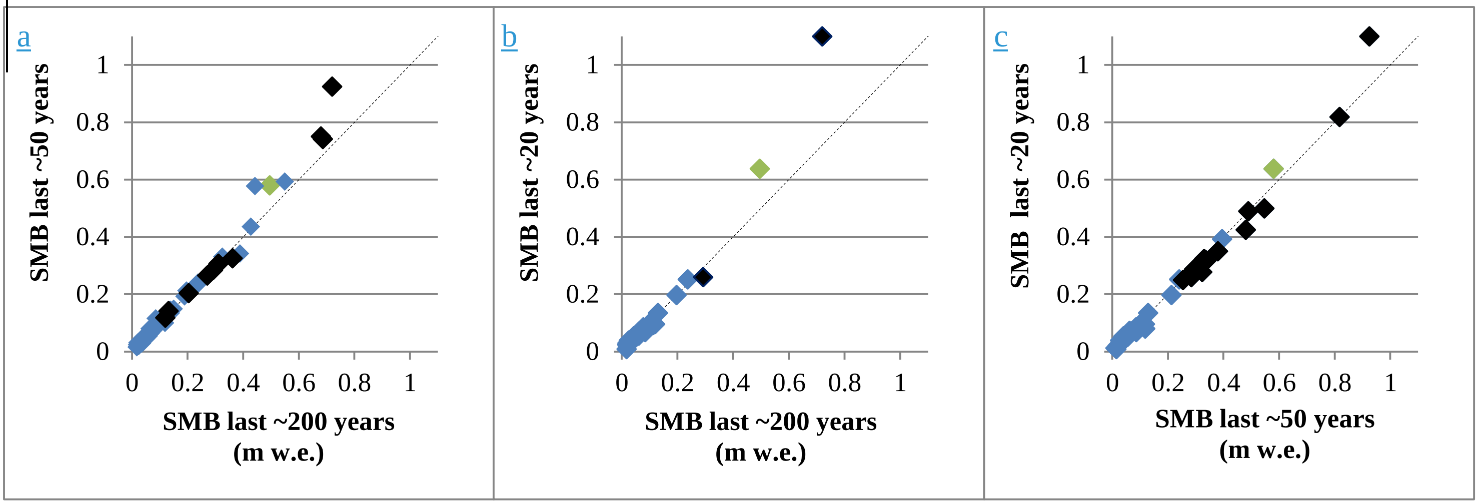

Fig. 9. Comparison of SMB between~~:~~ different periods reconstructed for ice cores from the continent (see Table A1 for site location, references and exact periods): (a) the last ~200 years and the last ~50 years; (b) the last ~200 years and the last ~20 years; (c) the last ~50 years and the last ~20 years. ~~See Table A1 for exact periods.~~ Coastal sites (< 1500 m a.s.l. and < 100 km away from the ice shelf) are shown in black, with the exception of our study site, IC12, which is shown in green. Inland sites are shown in blue. The 1:1 slope (0 % change) is shown as a dotted line.

Supplementary materials

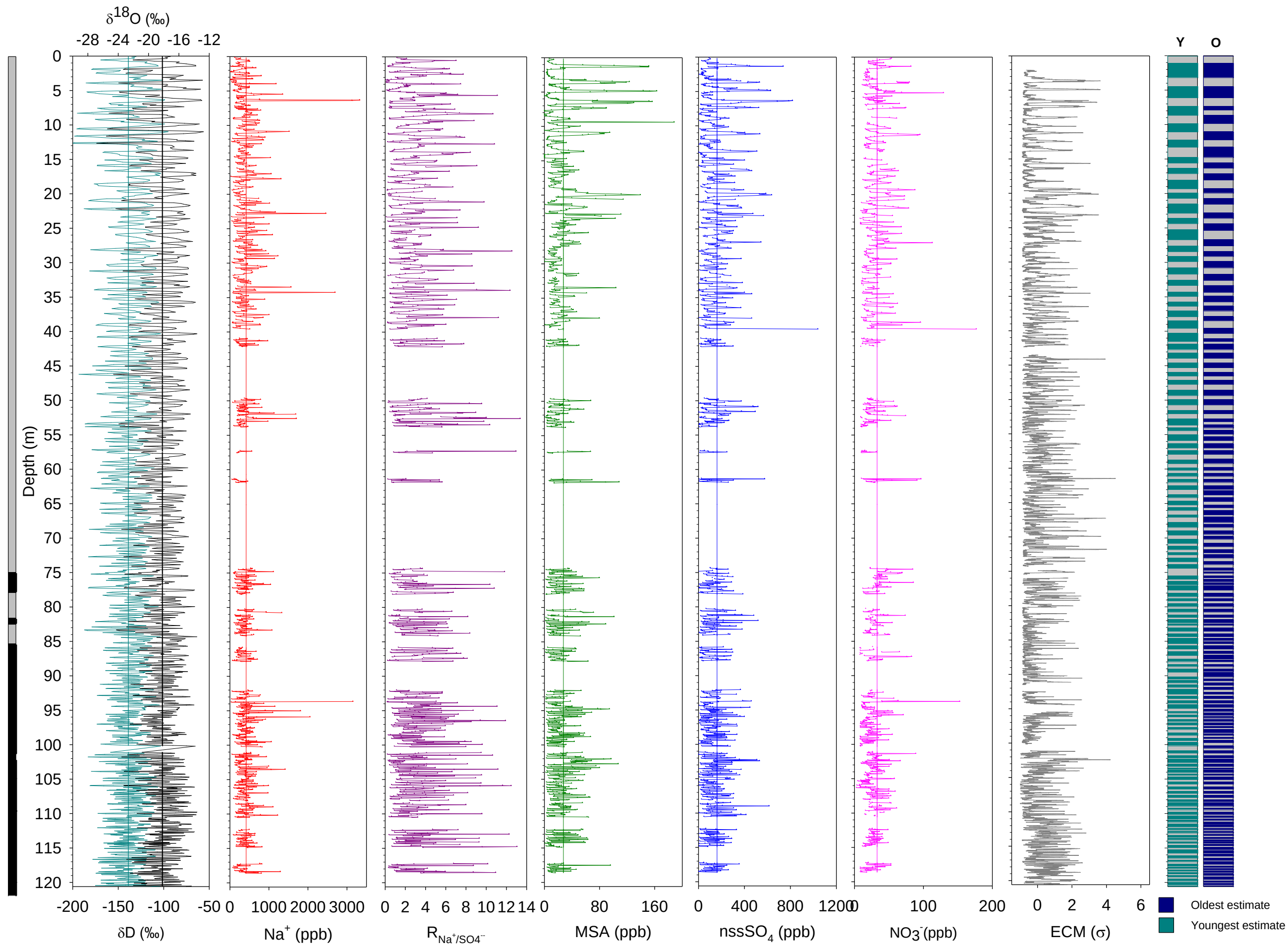

Fig. S1. Full vertical profile of water stable isotopes with, from left to right: a grey and black band indicating sections of sampling for major ions at 10 cm and 5 cm resolution, respectively; water stable isotopes, major ions andtaken at 5 cm resolution for the entire core; major ions, taken at 5 cm resolution for discrete sections; normalized ECM conductivity (0.05 m running mean, expressed as multiple of standard deviation (, σ) (light grey: 1 mm resolution, dark grey: 0.05 m running mean). The 4σ threshold is shown as a dotted vertical line, and identified volcanic peaks as dashed grey horizontal lines;); annual layer boundaries in the youngest (Green) and the oldest (Blue) estimates. Each (each colour transition indicates a boundary.).

Fig. S2. Full vertical profile, as in Fig. S1 but split in 17 sections for more visibility.

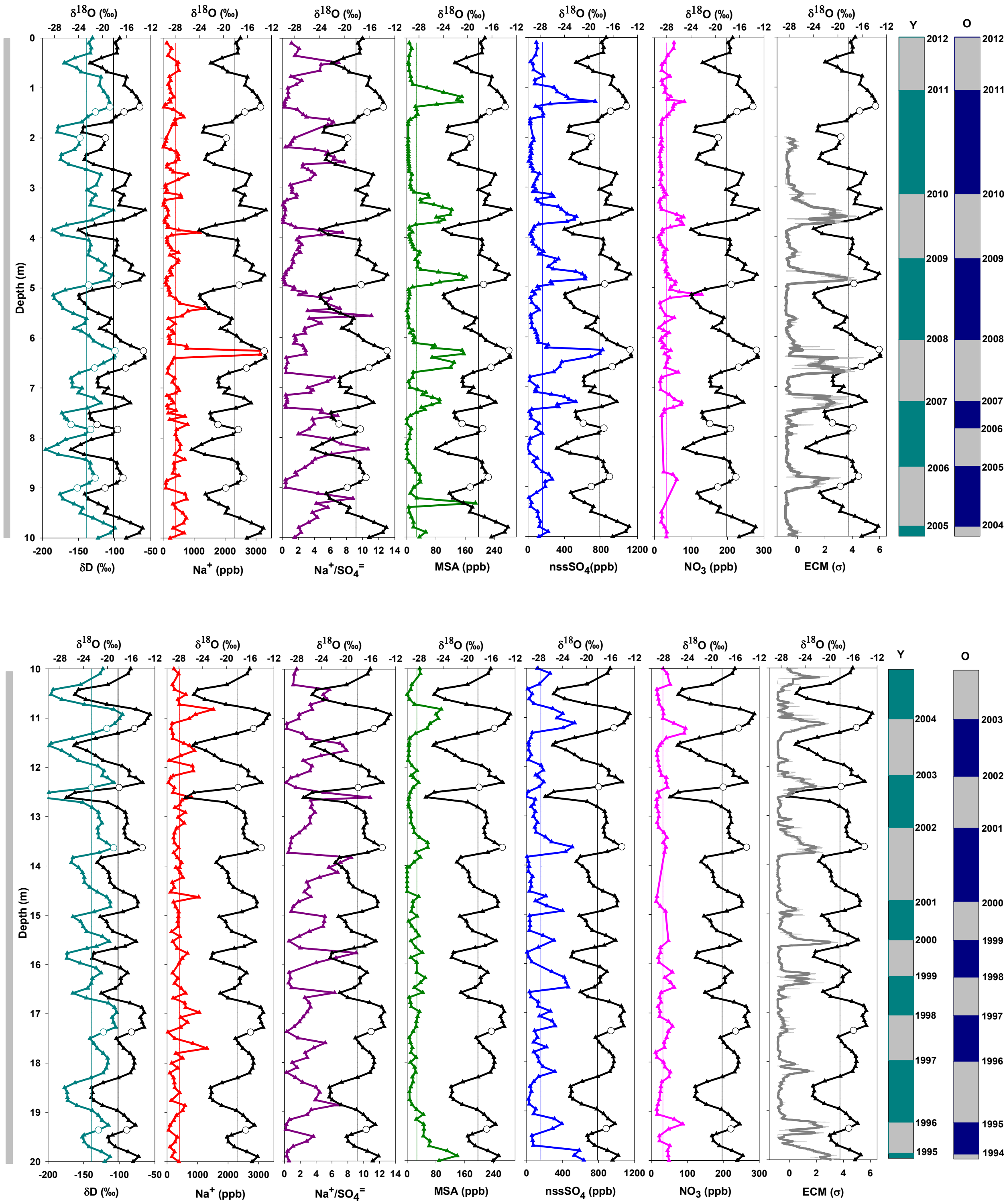

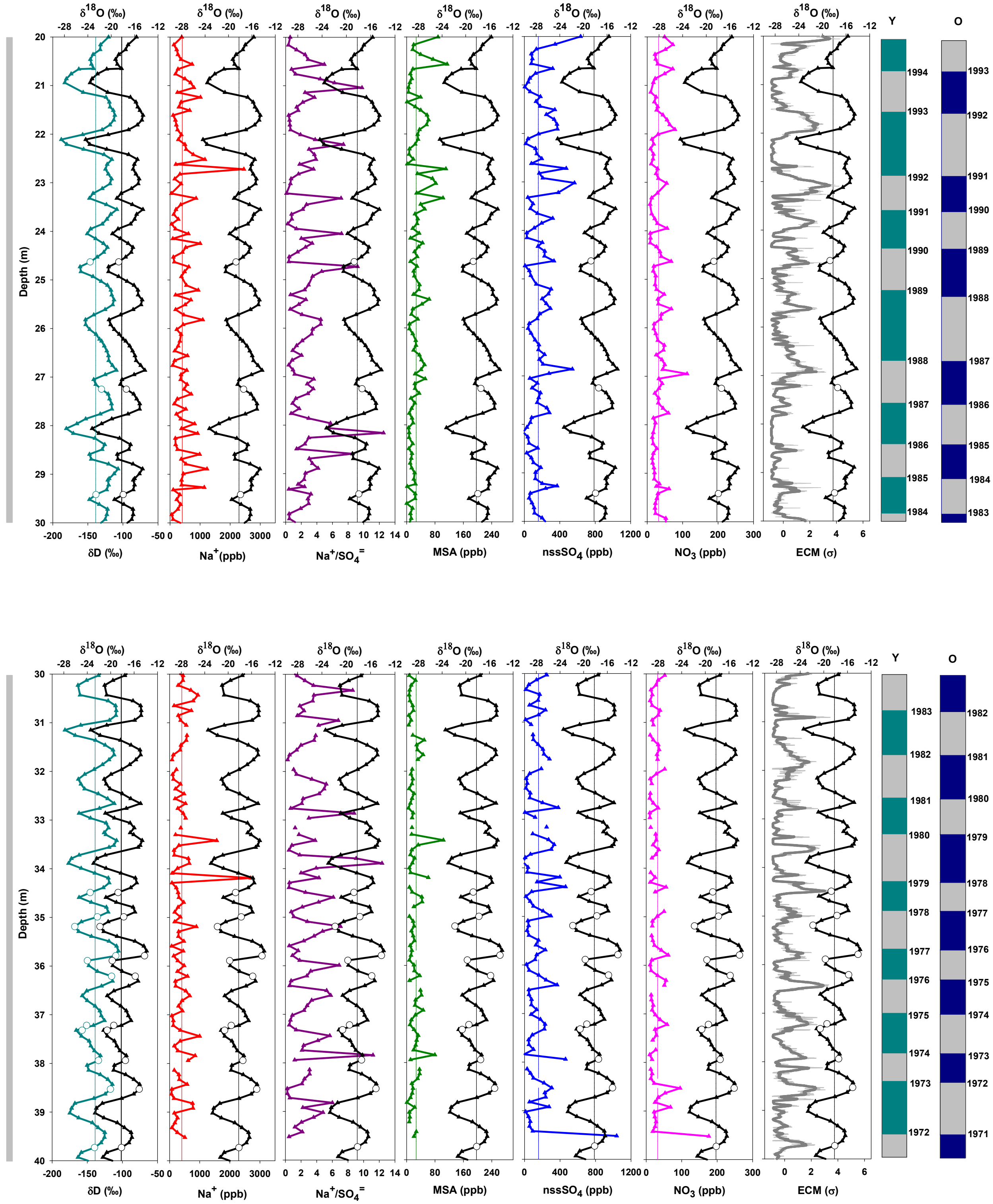
δ18O (‰)
Depth (m)
δD (‰)
Na+(ppb)
Na+/SO4=
MSA (ppb)
nssSO4 (ppb)
NO3 (ppb)
ECM (σ)
Y
O
1994
1993
1992
1991
1990
1989
1988
1987
1986
1985
1984
1983
1982
1981
1980
1979
1978
1977
1976
1975
1974
1973
1972
1971

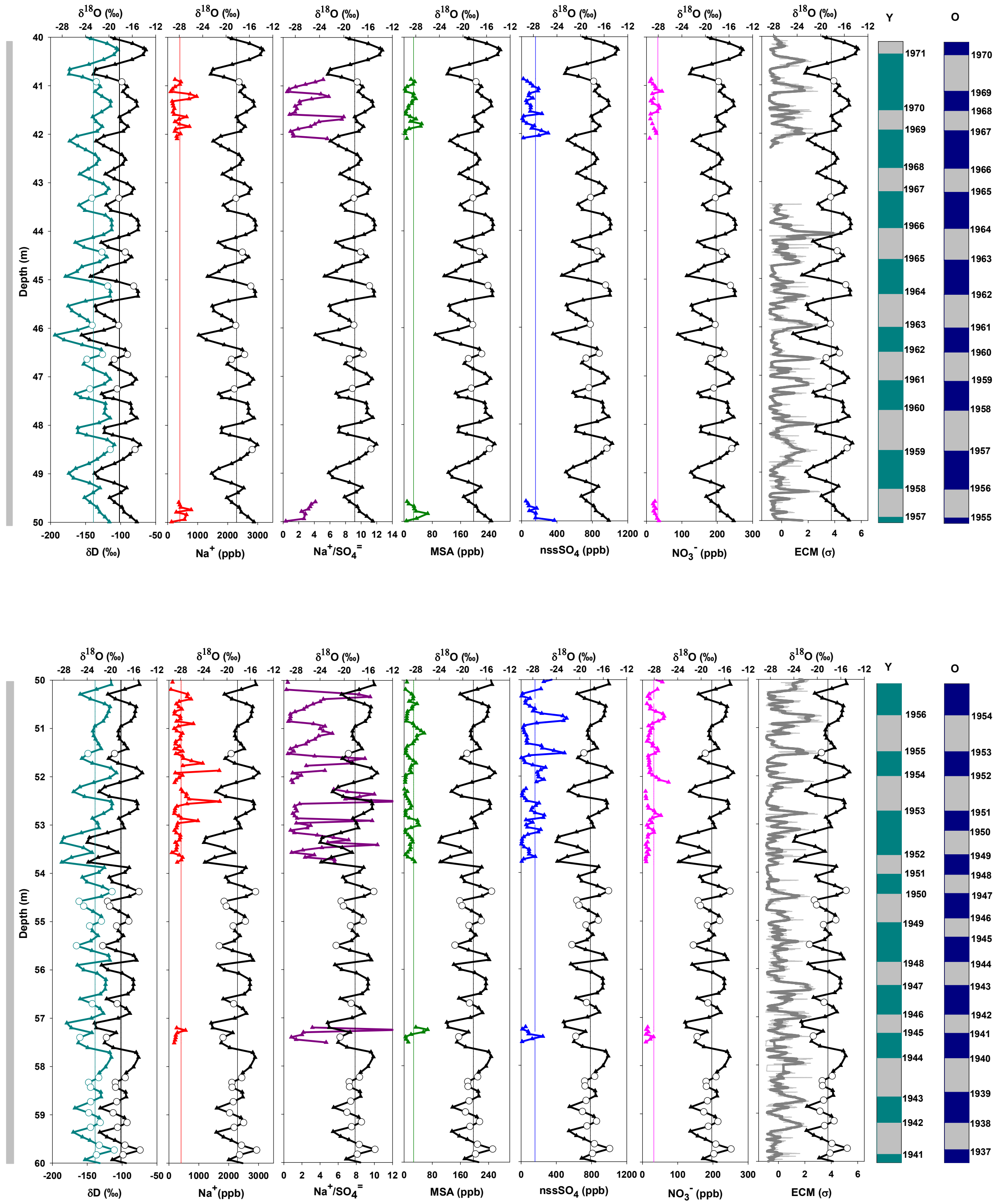
δ18O (‰)
Depth (m)
δD (‰)
Na+ (ppb)
Na+/SO4=
MSA (ppb)
nssSO4 (ppb)
NO3- (ppb)
ECM (σ)
Y
O
1971
1970
1969
1968
1967
1966
1965
1964
1963
1962
1961
1960
1959
1958
1957
1956
1955
1954
1953
1952
1951
1950
1949
1948
1947
1946
1945
1944
1943
1942
1941
1940
1939
1938
1937

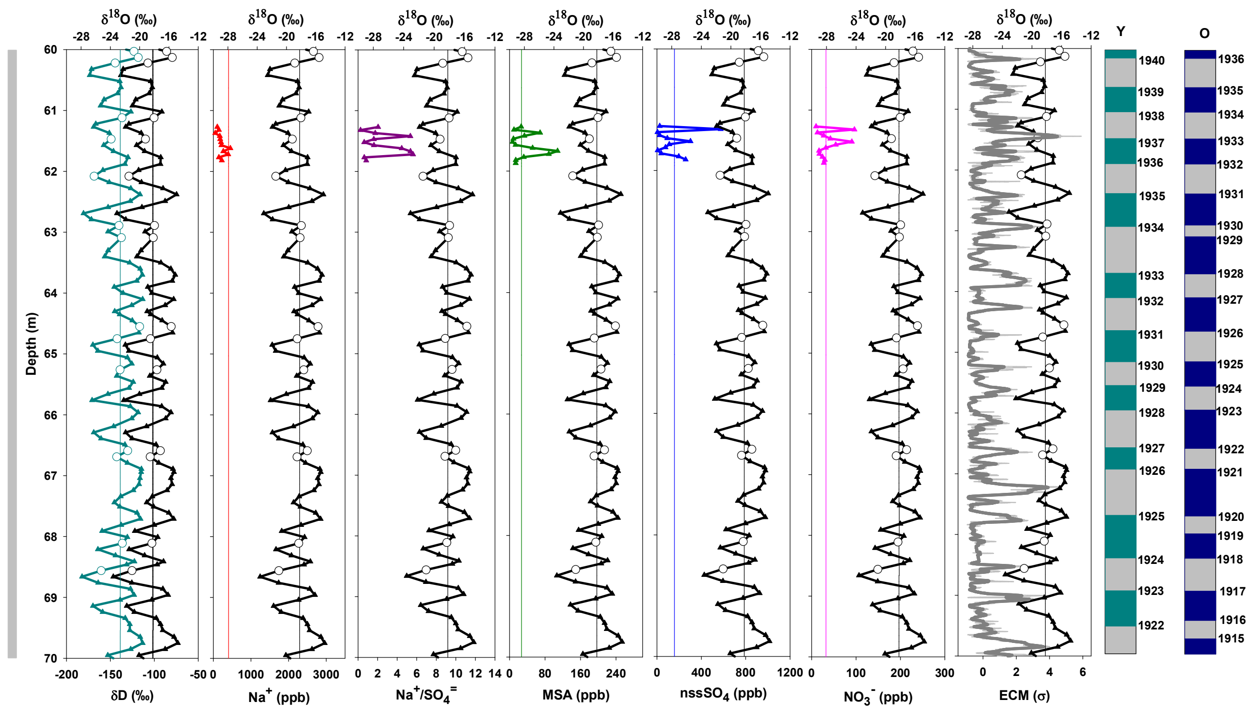
δ18O (‰)
Depth (m)
δD (‰)
Na+ (ppb)
Na+/SO4=
MSA (ppb)
nssSO4 (ppb)
NO3- (ppb)
ECM (σ)
Y
O
1940
1939
1938
1937
1936
1935
1934
1933
1932
1931
1930
1929
1928
1927
1926
1925
1924
1923
1922
1936
1935
1934
1933
1932
1931
1930
1929
1928
1927
1926
1925
1924
1923
1922
1921
1920
1919
1918
1917
1916
1915

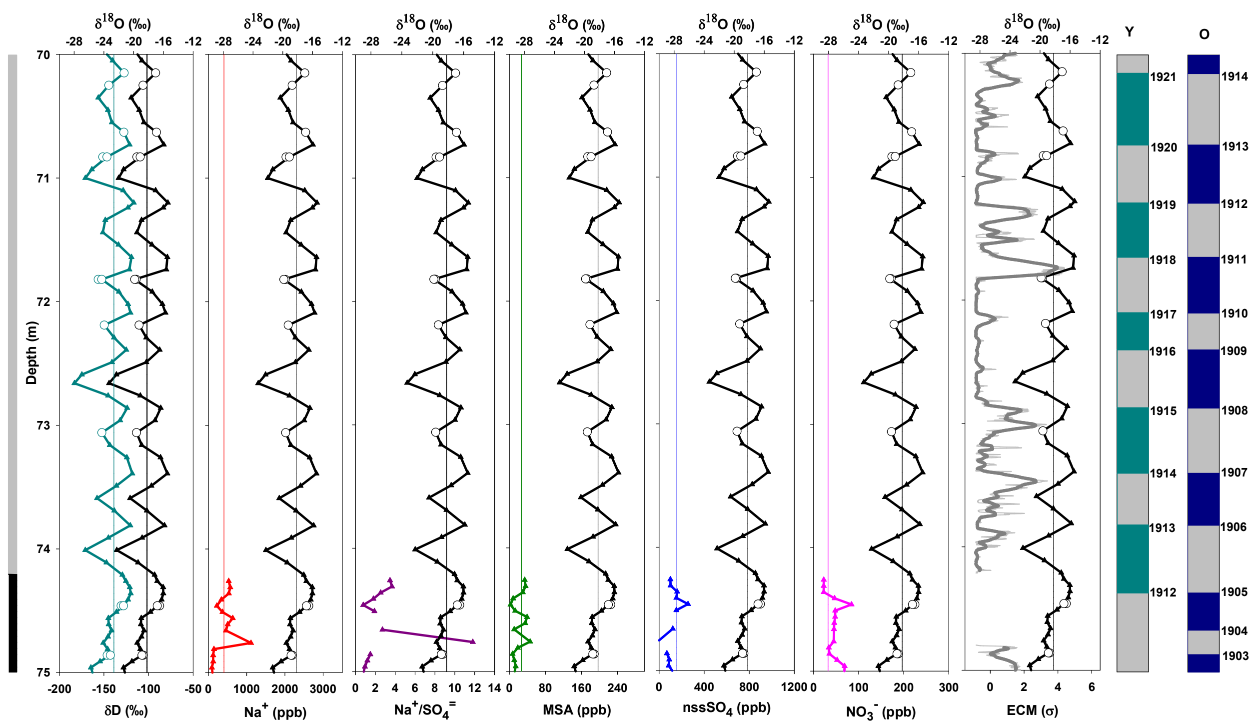
δ18O (‰)
Depth (m)
δD (‰)
Na+ (ppb)
Na+/SO4=
MSA (ppb)
nssSO4 (ppb)
NO3- (ppb)
ECM (σ)
Y
O
1921
1920
1919
1918
1917
1916
1915
1914
1913
1912
1914
1913
1912
1911
1910
1909
1908
1907
1906
1905
1904
1903

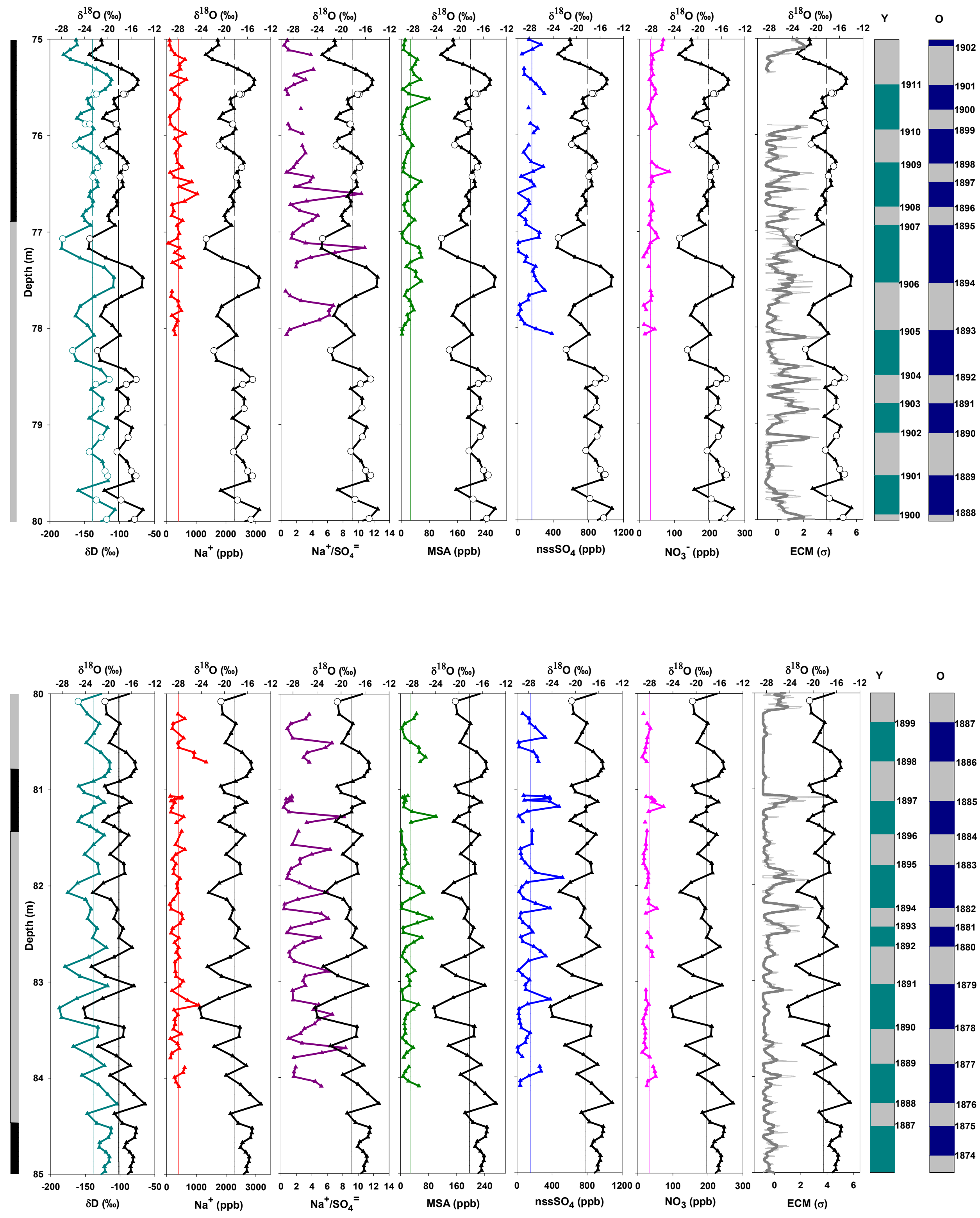

δ18O (‰)
-28 -24 -20 -16 -12
Depth (m)
75
76
77
78
79
80
-200 -150 -100 -50
δD (‰)
0 1000 2000 3000
Na+ (ppb)
0 2 4 6 8 10 12 14
Na+/SO4=
0 80 160 240
MSA (ppb)
0 400 800 1200
nssSO4 (ppb)
0 100 200 300
NO3- (ppb)
0 2 4 6
ECM (σ)
Y
1911
1910
1909
1908
1907
1906
1905
1904
1903
1902
1901
1900
O
1902
1901
1900
1899
1898
1897
1896
1895
1894
1893
1892
1891
1890
1889
1888
81
82
83
84
85
NO3 (ppb)
1899
1898
1897
1896
1895
1894
1893
1892
1891
1890
1889
1888
1887
1887
1886
1885
1884
1883
1882
1881
1880
1879
1878
1877
1876
1875
1874

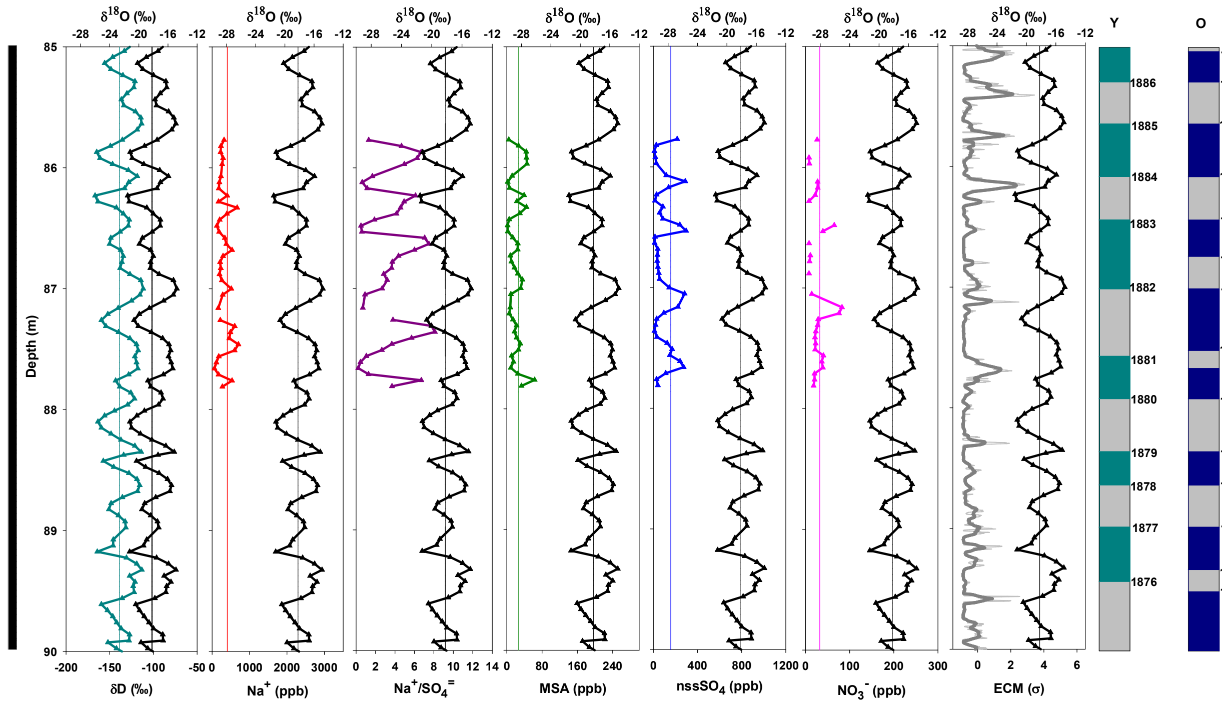
δ18O (‰)
Depth (m)
δD (‰)
Na+ (ppb)
Na+/SO4=
MSA (ppb)
nssSO4 (ppb)
NO3- (ppb)
ECM (σ)
Y
O
1886
1885
1884
1883
1882
1881
1880
1879
1878
1877
1876
1873
1872
1871
1870
1869
1868
1867
1866
1865
1864
1863
1862
1861
1860
1859

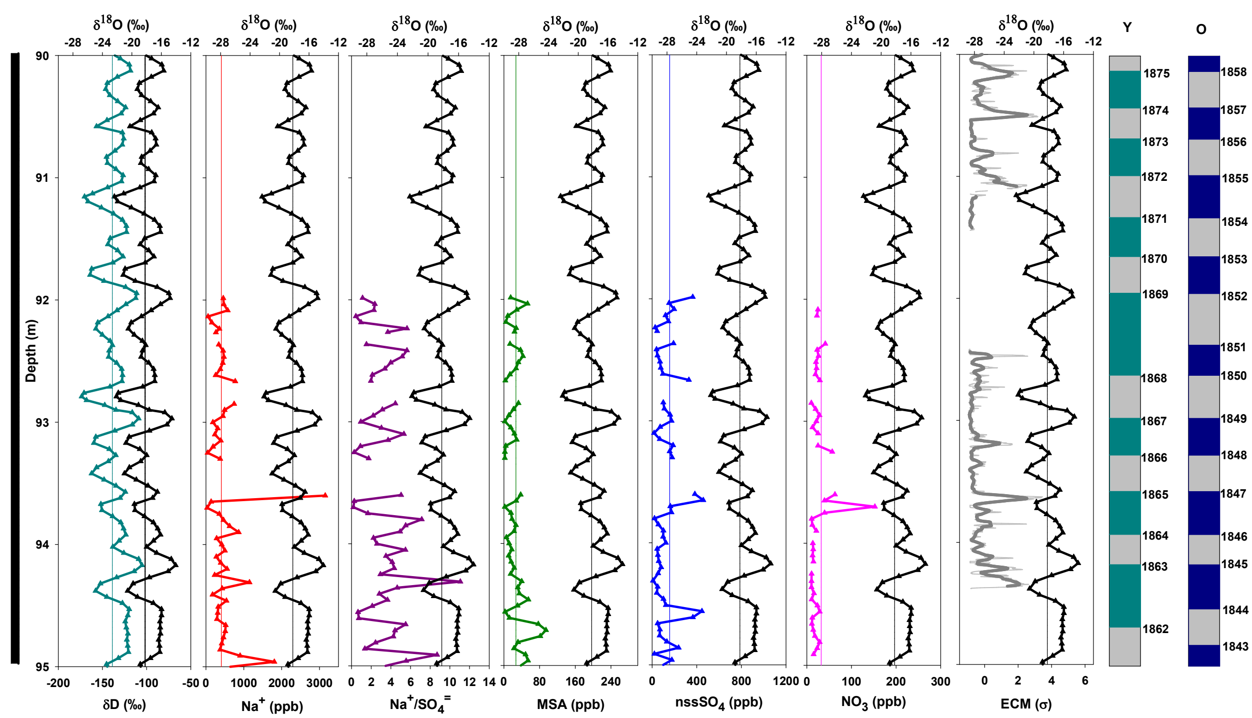
δ18O (‰)
Depth (m)
δD (‰)
Na+ (ppb)
Na+/SO4=
MSA (ppb)
nssSO4 (ppb)
NO3 (ppb)
ECM (σ)
Y
O
1875
1874
1873
1872
1871
1870
1869
1868
1867
1866
1865
1864
1863
1862
1858
1857
1856
1855
1854
1853
1852
1851
1850
1849
1848
1847
1846
1845
1844
1843

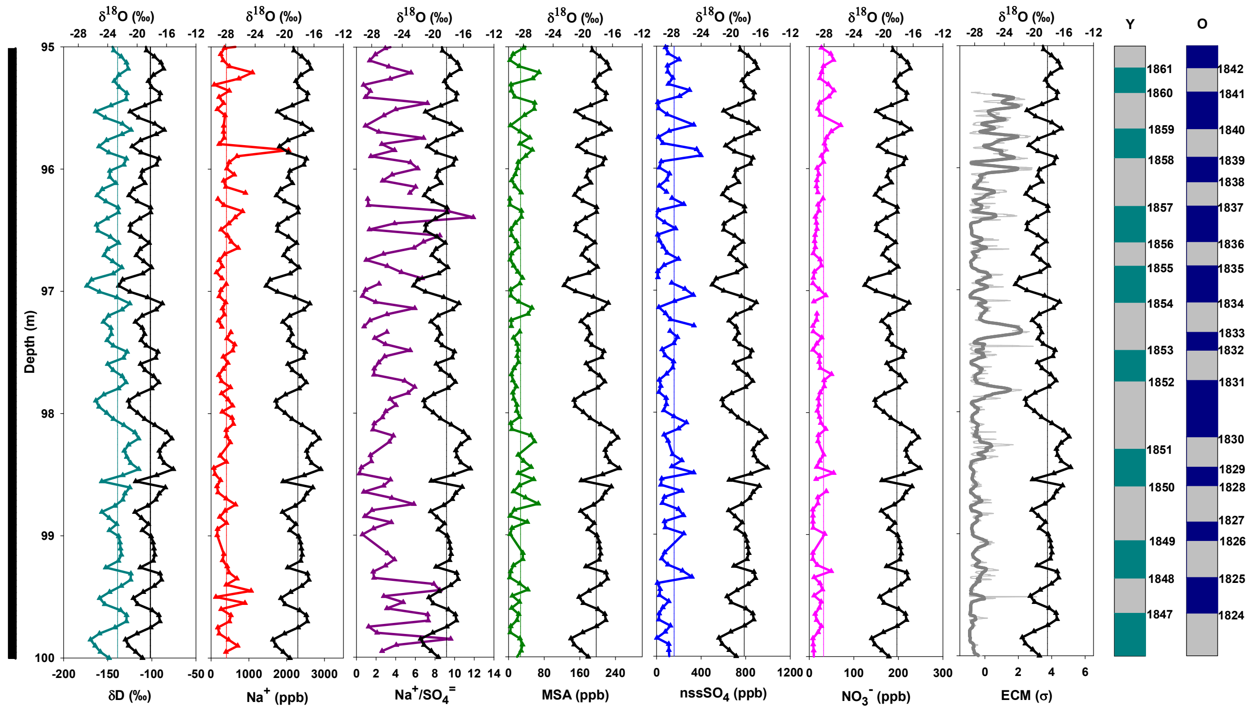
δ18O (‰)
Depth (m)
δD (‰)
Na+ (ppb)
Na+/SO4=
MSA (ppb)
nssSO4 (ppb)
NO3- (ppb)
ECM (σ)
Y
O
1861
1860
1859
1858
1857
1856
1855
1854
1853
1852
1851
1850
1849
1848
1847
1842
1841
1840
1839
1838
1837
1836
1835
1834
1833
1832
1831
1830
1829
1828
1827
1826
1825
1824

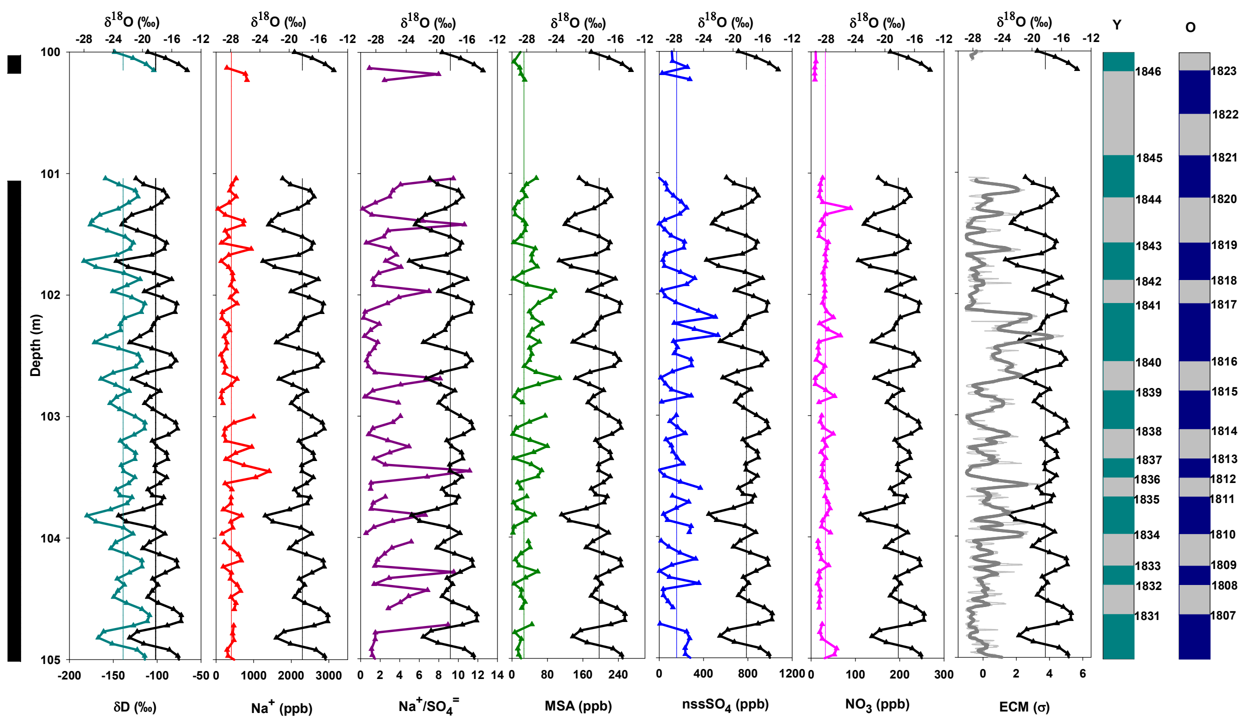
δ18O (‰)
Depth (m)
δD (‰)
Na+ (ppb)
Na+/SO4=
MSA (ppb)
nssSO4 (ppb)
NO3 (ppb)
ECM (σ)
Y
O
1846
1845
1844
1843
1842
1841
1840
1839
1838
1837
1836
1835
1834
1833
1832
1831
1823
1822
1821
1820
1819
1818
1817
1816
1815
1814
1813
1812
1811
1810
1809
1808
1807

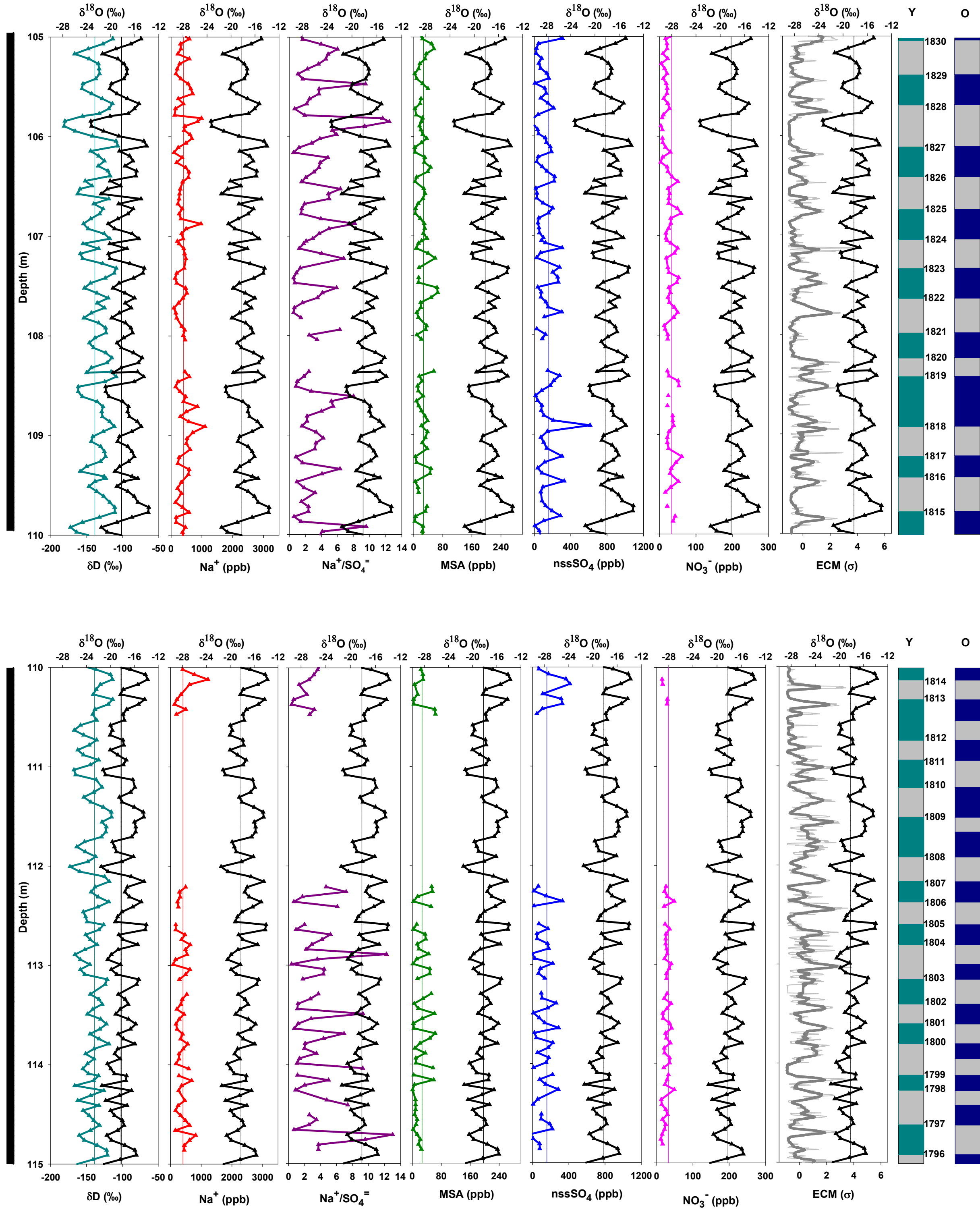

δ18O (‰)
-28 -24 -20 -16 -12
105
106
107
108
109
110
Depth (m)
-200 -150 -100 -50
δD (‰)
0 1000 2000 3000
Na+ (ppb)
0 2 4 6 8 10 12 14
Na+/SO4=
0 80 160 240
MSA (ppb)
0 400 800 1200
nssSO4 (ppb)
0 100 200 300
NO3- (ppb)
0 2 4 6
ECM (σ)
Y
1830
1829
1828
1827
1826
1825
1824
1823
1822
1821
1820
1819
1818
1817
1816
1815
O
1806
1805
1804
1803
1802
1801
1800
1799
1798
1797
1796
1795
1794
1793
1792
1791
δ18O (‰)
-28 -24 -20 -16 -12
110
111
112
113
114
115
Depth (m)
-200 -150 -100 -50
δD (‰)
0 1000 2000 3000
Na+ (ppb)
0 2 4 6 8 10 12 14
Na+/SO4=
0 80 160 240
MSA (ppb)
0 400 800 1200
nssSO4 (ppb)
0 100 200 300
NO3- (ppb)
0 2 4 6
ECM (σ)
Y
1814
1813
1812
1811
1810
1809
1808
1807
1806
1805
1804
1803
1802
1801
1800
1799
1798
1797
1796
O
1790
1789
1788
1787
1786
1785
1784
1783
1782
1781
1780
1779
1778
1777
1776
1775
1774
1773
1772
1771
1770
1769
1768
1767

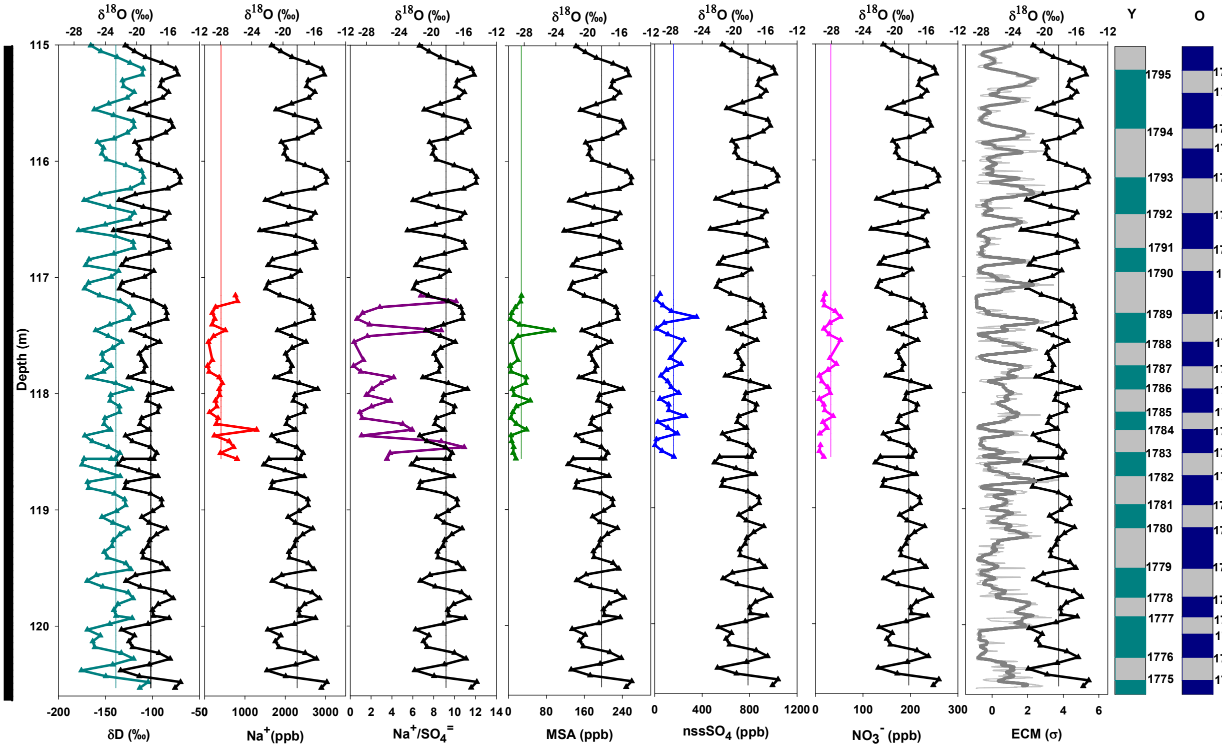

δ18O (‰)
Depth (m)
δD (‰)
Na+(ppb)
Na+/SO4=
MSA (ppb)
nssSO4 (ppb)
NO3- (ppb)
ECM (σ)
Y
O

Appendix A

Table A1. Sites information and SMB values *no significant trend during the 20th century **short record: only recent periods are compared ***when only a stacked SMB change is given, SMB from individual ice cores are inferred from the stacked record as if it was the same trend for all ice cores. Ref : reference period. Numbers in italic are inferred from the trend given in the referenced paper

Site name	Latitude	Longitude	Elevation (m a.s.l.)	Reference period	SMB (10^{-3} m w.e.) (kg m^{-2} a^{-1})		Recent period	SMB (10^{-3} m w.e.) (kg m^{-2} a^{-1})		Most recent period	SMB (10^{-3} m w.e.) (kg m^{-2} a^{-1})		% change (50a - ref)	% change (20a - ref) except**	Method	Study
Siple Dome	-81.6530	-148.9980	620	1890-1994	120		1922-1991	118					-1.67%		Ice core	Kaspari et al., 2004
ITASE00-5	-77.6830	-123.9950	1828	1716-2000	140		1922-1991	141					0.71%		Ice core	Kaspari et al., 2004
ITAE99-1	-80.6200	-122.6300	1350	1724-1998	139		1922-1991	146					5.04%		Ice core	Kaspari et al., 2004
ITASE00-4	-78.0830	-120.0800	1697	1799-2000	189		1922-1991	193					2.12%		Ice core	Kaspari et al., 2004
RIDS C	-80.0100	-119.4300	1530	1903-1995	112		*1970-1995*	*108.35*					*-3.26%*		Ice core	Kaspari et al., 2004
RIDS B	-79.4600	-118.0500	1603	1922-1995	150		*1970-1995*	*149.37*					*-0.42%*		Ice core	Kaspari et al., 2004
RIDS A	-78.7300	-116.3300	1740	1831-1995	235		1922-1991	234					-0.43%		Ice core	Kaspari et al., 2004
ITASE00-1	-79.3830	-111.2390	1791	1653-2001	220		1922-1991	222					0.91%		Ice core	Kaspari et al., 2004
ITASE01-2	-77.8430	-102.9100	1353	1890-2001	427		1922-1991	436					2.11%		Ice core	Kaspari et al., 2004
ITASE01-3	-78.1200	-95.6460	1633	1859-2001	325		1922-1991	331					1.85%		Ice core	Kaspari et al., 2004
ITASE01-5	-77.0590	-89.1370	1246	1780-2001	388		1922-1991	342					-11.86%		Ice core	Kaspari et al., 2004
ITASE01-6	-76.0970	-89.0170	1232	**			1978-1990	395		*1978-1999*	*392.6*		*-0.61%*		Ice core	Kaspari et al., 2004
Gomez	-73.5900	-70.3600	1400	1855-2006	720		1970s-2006	925		1997-2006	1100		28.47%	53%	Ice core	Thomas et al., 2008
Dyer Plateau	-70.6700	-64.8900	2002	1790-1989	549		1969-1989	593					8.00%		Ice core	Raymond et al., 1996
James Ross Island	-64.2200	-57.6800	1640	1847-1980	443		1964-1990	578					30.47%		Ice core	Aristarain et al., 2004
R1	-78.3075	-46.2728	718	1816-1998	204	±7	*	*204*					0.00%		Ice core	Mulvaney et al., 2002
Berkner B25	-79.5700	-45.7200	890	1816-1956	131		1965-1994	141					7.63%		Ice core	Ruth et al., 2004
A	-72.6500	-16.6333	60	**			1975-1989	380		1980-1989	350			-8%	Ice core	Isaksson & Melvold, 2002
E	-73.6000	-12.4333	700	**			1932-1991	324		1980-1991	277			-15%	Ice core	Isaksson & Melvold, 2002; Isaksson et al., 1996
B39	-71.4100	-9.9000	655	**			1935-2007	818		*1987-2007*	*818*			0.00%	Ice core	Fernandoy et al., 2010
FB0704	-72.0600	-9.5600	760	**			1962-2007	489		*1987-2007*	*489*			0.00%	Ice core	Fernandoy et al., 2010
BAS-depot	-77.0333	-9.5000	2176	1816-1997	*71*		1965-1997	*71*					*0.00%*		Ice core	Hofstede et al., 2004
B04	-70.6200	-8.3700	35	1892-1981	362	±95	1960-1980	*325*					-10.22%			Schlosser & Oerter, 2002
CV	-76.0000	-8.0500	2400	1816-1997	62		1965-1997	68	±2	1992-1997	70		9.68%	13%	Ice core	Karlof et al., 2005
B38	-71.1600	-6.7000	690	**			1960-2007	1257		*1987-2007*	*1257*			0.00%	Ice core	Fernandoy et al., 2010
FB0702	-71.5700	-6.6700	539	**			1959-2007	547		*1987-2007*	*500*			-9%	Ice core	Fernandoy et al., 2010
FB9816	-75.0000	-3.5037	2740	1800-1997	47	±17	1950-1997	*51.5****					*9.57%*		Ice core	Oerter et al., 2000
B31	-75.5800	-3.4300	2669	1816-1997	58.4		1966-1989	59.8					2.40%		Ice core	Oerter et al., 2000
H	-70.5000	-2.4500	53	**			1953-1993	480		1980-1993	425			-11%	Ice core	Isaksson & Melvold, 2002
NUS08-2	-87.8500	-1.8000	2583	1815-2007/8	67.4	±2.6	1963-2007/8	63.4	±4.2				-5.93%		Ice core	Anschutz et al., 2011
S32	-70.3100	-0.8000	53	**			1995-2009	339	±36		*318*			-6%	Ice core	Schlosser et al., 2014
G3	-69.8230	-0.6120	57	**			1993-2009	295	±29		*288*			-2%	Ice core	Schlosser et al., 2014
FB9815	-74.9492	-0.5055	2840	1801-1997	59	±24	1950-1997	*65****					*10.17%*		Ice core	Oerter et al., 2000
G4	-70.9020	-0.4020	60	**			1983-2009	330	±21		*323*			-2%	Ice core	Schlosser et al., 2014
M2	-70.3160	-0.1090	73	**			1981-2009	315	±22		*302*			-4%	Ice core	Schlosser et al., 2014
G5	-70.5450	-0.0410	82	**			1983-2009	298	±21		*290*			-3%	Ice core	Schlosser et al., 2014
K	-70.7500	0.0000	53	**			1954-1996	254		1980-1996	250			0%	Ice core	Isaksson & Melvold, 2002
SPS	-90.0000	0.0000	2850	1816-1956	76.5		1965-1994	84.8	±3.3	1992-1997	84.5	±8.9	10.85%	10%	Ice core and poles	Mosley & Thompson, 1999
B32	-75.0023	0.0070	2882	1816-1997	63		1966-1997	80					26.98%		Ice core	Oerter et al., 2000
EPICA DML	-75.0020	0.0680	2774	1915-2008	73		1964-2008	73.1	±1.7				0.14%		Firn core and radar	Fujita et al., 2011
FB9808	-74.7507	0.9998	2860	1801-1997	68	±22	1950-1997	*74.5****					*9.56%*		Ice core	Oerter et al., 2000
FB9809	-74.4992	1.9608	2843	1801-1997	89	±29	1950-1997	*97.5****					*9.55%*		Ice core	Oerter et al., 2000
EPICA (Amundsenisen)	-75.0000	2.0000	2900	1865-1965	78		1966-1991	76					-2.56%		Ice core	Isaksson et al., 1996
G8	-70.4100	2.0100	58	**			1991-2009	282	±26		273			-3%	Ice core	Schlosser et al., 2014

Site name	Latitude	Longitude	Elevation (m a.s.l.)	Reference period	SMB (10^{-3} m w.e.) (kg m^{-2} a^{-1})		Recent period	SMB (10^{-3} m w.e.) (kg m^{-2} a^{-1})		Most recent period	SMB (10^{-3} m w.e.) (kg m^{-2} a^{-1})		% change (50a - ref)	% change (20a - ref) except**	Method	Study
FB9814	-75.0837	2.5017	2970	1801-1997	64	±21	1950-1997	71***					10.94%		Ice core	Oerter et al., 2000
C	-72.2583	2.8911	2400	1955-1996	119		1965-1996	123					3.36%		Ice core	Isaksson et al., 1999
D	-72.5083	3.0000	2610	1955-1996	112		1965-1996	116					3.57%		Ice core	Isaksson et al., 1999
DML08	-75.7528	3.2828	2971	1919-96	60	±19	*	60					0.00%		Ice core	Oerter et al., 1999
E	-72.6750	3.6628	2751	1955-1996	55		1965-1996	59					7.27%		Ice core	Isaksson et al., 1999
DML02	-74.9683	3.9185	3027	1919-95	59	±14	*	59					0.00%		Ice core	Oerter et al., 1999
FB9810	-74.6672	4.0017	2980	1801-1997	86	±29	1950-1997	94.5***					9.88%		Ice core	Oerter et al., 2000
F	-72.8583	4.3514	2840	1955-1996	23		1965-1996	24					4.35%		Ice core	Isaksson et al., 1999
S100	-70.2333	4.8000	48	1816-2000	292		1956-2000	284		1991-2000	260	±80	-2.74%	-11%	Ice core	Kaczmarska et al., 2004
S20	-70.2417	4.8111	63	1955-1996	271		1965-1996	265					-2.21%		Ice core	Isaksson et al., 1999
FB0601	-75.2470	4.8440	3090	1915-2008	52		1964-2008	51.6	±1.2				-0.77%		Firn core and radar	Fujita et al., 2011
FB9813	-75.1673	5.0033	3100	1816-1997	48		1950-1997	53***					10.42%		Ice core	Oerter et al., 2000
G	-73.0417	5.0442	2929	1955-1996	28		1965-1996	30					7.14%		Ice core	Isaksson et al., 1999
FB9804	-75.2503	6.0000	2630	1801-1997	50	±16	1950-1997	55***					10.00%		Ice core	Oerter et al., 2000
H	-73.3917	6.4606	3074	1955-1996	44		1965-1996	46					4.55%		Ice core	Isaksson et al., 1999
B33	-75.1670	6.4985	3160	1816-1997	45.9		1966-1989	55					19.83%		Ice core	Oerter et al., 2000, Sommer et al., 2000
FB9811	-75.0840	6.5000	3160	1801-1997	58	±16	1950-1997	64***					10.34%		Ice core	Oerter et al., 2000
DML09	-75.9333	7.2130	3156	1897-1996	45	±12	*	45					0.00%		Ice core	Oerter et al., 1999
DML10	-75.2167	7.2130	3364	1900-96	47	±11	*	47					0.00%		Ice core	Oerter et al., 1999
DML04	-74.3990	7.2175	3179	1905-1996	53	±15	*	53					0.00%		Ice core	Oerter et al., 1999
I	-73.8008	7.9406	3174	1955-1996	52		1965-1996	53					1.92%		Ice core	Isaksson et al., 1999
NUS07-1	74.7200	7.9800	3174	1815–2007/8	52	±2	1963–2007/08	55.9	±3.9				7.50%		Ice core	Anschutz et al., 2009
Site I	-73.7167	7.9833	3174	1815-2007	52	±1.3	1963-2007	56	±4.7	1991-2007	52		7.69%	0%	Ice core	Anschutz et al., 2009
DML06	-75.0007	8.0053	3246	1899-1996	50	±14	*	50					0.00%		Ice core	Oerter et al., 1999
NUS08-6	-81.7000	8.5700	2447	1815-2007/8	39.2	±1.5	1963-2007/8	49.2	±3.4				25.51%		Ice core	Anschutz et al., 2011
J	-74.0417	9.4917	3268	1955-1996	44		1965-1996	45	±4				2.27%		Ice core	Isaksson et al., 1999
FB0603	-75.1170	9.7240	3300	1915-2008	41		1964-2008	38	±0.9				-7.32%		Firn core and radar	Fujita et al., 2011
K	-74.3583	11.1036	3341	1955-1996	45		1965-1996	41					-8.89%		Ice core	Isaksson et al., 1999
L	-74.6417	12.7908	3406	1955-1996	45		1965-1996	41					-8.89%		Ice core	Isaksson et al., 1999
A28	-74.8617	14.7420	3466	1915-2008	44		1964-2008	44.5	±1				1.14%		Firn core and radar	Fujita et al., 2011
MC	-75.0112	14.8865	3470.4	1816-1884	40		1955-2000	39		1992-2000	46		-2.50%	15%	Ice core	Karlof et al., 2005
MD	-74.9706	14.9567	3470.8	1816-1884	42		1955-2000	40		1992-2000	53		-4.76%	26%	Ice core	Karlof et al., 2005
M	-75.0000	14.9964	3470	1816-1884	41	±0.7	1955-2000	41	±0.5	1992-2000	50	±1.1	0.00%	22%	Ice core	Karlof et al., 2005
M150	-74.9900	15.0000	3470	1816-1997	43		1965-1997	48.5					12.79%		Ice core	Hofstede et al., 2004
M	-74.9917	15.0017	3453	1955-1965	51		1965-1996	45					-11.76%		Ice core	Isaksson et al., 1999
MB	-75.0294	15.0435	3470.5	1816-1884	39		1955-2000	42		1992-2000	46		7.69%	18%	Ice core	Karlof et al., 2005
MA	-74.9887	15.1134	3470.4	1816-1884	42		1955-2000	42		1992-2000	48	±1.3	0.00%	14%	Ice core	Karlof et al., 2005
NUS08-5	-82.6300	17.8700	2544	1815-2007/8	35	±0.8	1963-2007/8	37.6	±2.3				7.43%		Ice core	Anschutz et al., 2011
NUS08-4	-82.8167	18.9000	2552	1815-2007/8	36.7	±0.9	1963-2007/8	36.1	±2.1				-1.63%		Ice core	Anschutz et al., 2011
NUS08-3	-84.1300	22.0000	2625	1815-2007/8	40.1	±1	1963-2007/8	45.3	±3.1				12.97%		Ice core	Anschutz et al., 2011
A35	-76.0660	22.4590	3586	1915-2008	35		1964-2008	39.2	±0.9				12.00%		Firn core and radar	Fujita et al., 2011
NUS07-2	-76.0700	22.4700	3582	1815-2007/8	33	±0.7	1963-2007/8	28	±2				-15.15%		Ice core	Anschutz et al., 2011
MP	-75.8880	25.8340	3661	1286-2008	33.1	±1.0	1964-2008	38.7	±0.9	1993-2008	41.9	±2.8	16.92%	27%	Firn core and radar	Fujita et al., 2011
NUS07-3	-77.0000	26.0500	3589	1815-2007/8	22	±0.5	1963-2007/8	23.7	±1.7				7.73%		Ice core	Anschutz et al., 2009
IC12	-70.2458	26.3349	450	1816-2012	480	±10	1955-2012	630	±20	1992-2012	680	±70	31.25%	42%	Ice core	This paper
DK190	-76.7940	31.9000	3741	1286-2008	28.7	± 0.9				1993-2008	34.1	±2.3		19%	Firn core and radar	Fujita et al., 2011
NUS07-4	-78.2167	32.8500	3595	1815-2007/8	19	±0.5	1963-2007/8	17.5	±1.2				-7.89%		Ice core	Anschutz et al., 2009
NUS07-5	-78.6500	35.6300	3619	1815-2007/8	24	±0.5	1963-2007/8	20.1	±1.4				-16.25%		Ice core	Anschutz et al., 2011

Site name	Latitude	Longitude	Elevation (m a.s.l.)	Reference period	SMB (10^{-3} m w.e.) (kg m^{-2} a^{-1})		Recent period	SMB (10^{-3} m w.e.) (kg m^{-2} a^{-1})		Most recent period	SMB (10^{-3} m w.e.) (kg m^{-2} a^{-1})		% change (50a - ref)	% change (20a - ref) except**	Method	Study
DF	-77.3170	39.7030	3810	1816-2001	26.3		1964-2008	28.8	±0.7	1995-2006	27.3	±0.4	9.51%	4%	Ice core	Igarashi et al., 2011
YM85	-71.5800	40.6300	2246	1816-2002	140		1965-2002	135					-3.57%		Ice core	Takahashi et al., 2009
H72	-69.2047	41.0906	1214	1831-1998	311		1973-1998	307					-1.29%		Ice core and poles	Nishio et al., 2002
NUS07-6	-80.7833	44.8500	3672	1815-2007/8	22		1902-2007/8	21					-4.55%		Ice core	Anschutz et al., 2009
G15	-71.2000	45.9800	2544	1816-1964	86		1964-1984	116					34.88%		Ice core	Moore et al., 1991
NUS07-8	-84.1833	53.5333	3452	1815-2007/8	32	±1.2	1963-2007/8	30	±2.1				-6.25%		Ice core	Anschutz et al., 2009
NUS07-7	-82.0700	54.5500	3725	1815-2007/8	29.4	±0.6	1963-2007/8	26.1	±1.9				-11.22%		Ice core	Anschutz et al., 2011
DT217	-75.7167	76.8333	2800	**			1998-2008	12	±1.72	2005-2008	12			0%	Stake arrays	Ding et al., 2011
DT364	-78.3333	77.0000	3380	**			1999-2008	62	±0.14	2005-2008	72			16%	Stake arrays	Ding et al., 2011
DT401	-79.0200	77.0000	3760	1816-1999	19		1963-1999	24		1999–2005	25	±16	26.32%	32%	Ice core	Ren et al., 2010; Ding et al., 2011a
DT001	-70.8300	77.0700	2325	1810-1959	131		1959-1996	131					0.00%		Ice core	Zhang et al., 2006
Dome A	-80.3667	77.3500	4093	**			2005-2008	19	±0.25	2008-2009	21			11%	Stake arrays	Ding et al., 2011
DomeA	-80.3600	77.3600	4092	1815-1998	23		1963-1998	23					0.00%		Ice core	Jiang et al., 2012
LGB65	-71.8500	77.9200	1850	1815-1996	131		1960-1996	131					0.00%		Ice core	Xiao et al., 2004
DT008	-72.1667	77.9333	2390	**			1998-2008	118	±0.30	2005-2008	80			-32%	Stake arrays	Ding et al., 2011
VOSTOK	-78.4500	106.8300	3488	1816-2010	20.6	±0.3	1955-2010	21.5	±0.5	1958-2010	20.8		4.37%	1%	Snow pits and poles	Ekaykin et al., 2004
DSS	-66.7697	112.8069	1370	1816-2000	680		1970-2009	750					10.29%		Ice core	Roberts et al., 2015
LAW DOME	-66.7700	112.9800	1370	1816-1966	687		1966-2005	742					8.01%		Ice core	Morgan et al., 1991; van Ommen & Morgan, 2010
DomeC	-75.1200	123.3100	3233	1816-1998	25.3		1965-1998	28.3		1996-1998	39		11.86%	54%	Ice core and poles	Frezzotti et al., 2005
D6 A	-75.4400	129.8100	3027	1816-1998	36	±1.8	1966-1998	29	±1.4	1998-2002	39		-19.44%	8%	Ice core and poles	Frezzotti et al., 2005
D66	-68.9400	136.9400	2333	1966-1864	196		1965-2001	213	±13	2001-2003	197		8.67%	1%	Ice core and poles	Magand et al., 2004;Frezzotti et al., 2013
D2 A	-75.6200	140.6300	2479	1816-1998	20	±1.0	1966-1998	31	±1.6	1998-2002	30		55.00%	50%	Ice core and poles	Frezzotti et al., 2005
GV1	-70.8700	141.3800	2244	1816-2001	114		1965-2001	117	±7	2001-2003	96		2.63%	-16%	Ice core and poles	Magand et al., 2004;Frezzotti et al., 2013
GV2	-71.7100	145.2600	2143	1816-2001	112		1965-2001	112	±7	2001-2003	92		0.00%	-18%	Ice core and poles	Magand et al., 2004;Frezzotti et al., 2013
MdPtA	-75.5300	145.8600	2454	1816-1998	36	±1.8	1966-1998	45	±2.7	1998-2010	47		25.00%	31%	Ice core and poles	Frezzotti et al., 2005
GV3	-72.6300	150.1700	2137	1816-2001	81		1965-2001	84	±5	2001-2003	73		3.70%	-10%	Ice core and poles	Magand et al., 2004;Frezzotti et al., 2013
M2 A	-74.8000	151.2700	2278	1816-1998	17	±0.8	1966-1998	15	±7.5	1998-2002	8.5		-11.76%	-50%	Ice core and poles	Frezzotti et al., 2005
GV4	-72.3900	154.4800	2126	1816–2001	119		1965–2001	100	±6	2001–2003	96		-15.97%	-19%	Ice core and poles	Magand et al., 2004;Frezzotti et al., 2013
31DPT A	-74.0300	155.9600	2069	1816-1998	98	±4.9	1966-1998	112	±5.6	1998-2002	98		14.29%	0%	Ice core and poles	Frezzotti et al., 2005
GPS2A	-74.6400	157.5020	1804	1816-1998	60	±3.0	1966-1998	54	±2.7	1993-2000	55		-10.00%	-8%	Ice core and poles	Frezzotti et al., 2005
GV5	-71.8900	158.5400	2184	1816-2001	129		1965-2001	129	±7	2001-2004	135		0.00%	5%	Ice core and poles	Magand et al., 2004;Frezzotti et al., 2007
GV7	-70.6800	158.8600	1947	1854-2001	237		1965-2001	241	±13	2001-2004	252		1.69%	6%	Ice core and poles	Magand et al., 2004;Frezzotti et al., 2007
Talos Dome	-72.7700	159.0800	2316	1816-2001	83.6		1966-1996	86.6		2001-2010	68		3.59%	-19%	Ice core and poles	Magand et al., 2004;Frezzotti et al., 2007; 2013
Hercules Neve	-73.1000	165.4000	2960	1816-1966	118		1966-1992	129					9.32%		Ice core	Stenni et al., 1999